

Wilfrid Laurier University

Scholars Commons @ Laurier

---

Theses and Dissertations (Comprehensive)

---

1990

## Identifying directional properties of spatial point patterns an investigation of two methods

Rolf Puchtinger

*Wilfrid Laurier University*

Follow this and additional works at: <https://scholars.wlu.ca/etd>



Part of the [Geographic Information Sciences Commons](#), and the [Statistics and Probability Commons](#)

---

### Recommended Citation

Puchtinger, Rolf, "Identifying directional properties of spatial point patterns an investigation of two methods" (1990). *Theses and Dissertations (Comprehensive)*. 320.

<https://scholars.wlu.ca/etd/320>

This Thesis is brought to you for free and open access by Scholars Commons @ Laurier. It has been accepted for inclusion in Theses and Dissertations (Comprehensive) by an authorized administrator of Scholars Commons @ Laurier. For more information, please contact [scholarscommons@wlu.ca](mailto:scholarscommons@wlu.ca).



National Library  
of Canada

Bibliothèque nationale  
du Canada

Canadian Theses Service    Service des thèses canadiennes

Ottawa, Canada  
K1A 0N4

## NOTICE

The quality of this microform is heavily dependent upon the quality of the original thesis submitted for microfilming. Every effort has been made to ensure the highest quality of reproduction possible.

If pages are missing, contact the university which granted the degree.

Some pages may have indistinct print especially if the original pages were typed with a poor typewriter ribbon or if the university sent us an inferior photocopy.

Reproduction in full or in part of this microform is governed by the Canadian Copyright Act, R.S.C. 1970, c. C-30, and subsequent amendments.

## AVIS

La qualité de cette microforme dépend grandement de la qualité de la thèse soumise au microfilmage. Nous avons tout fait pour assurer une qualité supérieure de reproduction.

S'il manque des pages, veuillez communiquer avec l'université qui a conféré le grade.

La qualité d'impression de certaines pages peut laisser à désirer, surtout si les pages originales ont été dactylographiées à l'aide d'un ruban usé ou si l'université nous a fait parvenir une photocopie de qualité inférieure.

La reproduction, même partielle, de cette microforme est soumise à la Loi canadienne sur le droit d'auteur, SRC 1970, c. C-30, et ses amendements subséquents.



National Library  
of Canada

Bibliothèque nationale  
du Canada

Canadian Theses Service    Service des thèses canadiennes

Ottawa Canada  
K1A 0N4

The author has granted an irrevocable non-exclusive licence allowing the National Library of Canada to reproduce, loan, distribute or sell copies of his/her thesis by any means and in any form or format, making this thesis available to interested persons.

The author retains ownership of the copyright in his/her thesis. Neither the thesis nor substantial extracts from it may be printed or otherwise reproduced without his/her permission.

L'auteur a accordé une licence irrévocable et non exclusive permettant à la Bibliothèque nationale du Canada de reproduire, prêter, distribuer ou vendre des copies de sa thèse de quelque manière et sous quelque forme que ce soit pour mettre des exemplaires de cette thèse à la disposition des personnes intéressées.

L'auteur conserve la propriété du droit d'auteur qui protège sa thèse. Ni la thèse ni des extraits substantiels de celle-ci ne doivent être imprimés ou autrement reproduits sans son autorisation.

ISBN 0 515 53142-5

Canada

**Identifying Directional Properties of  
Spatial Point Patterns:  
An Investigation of Two Methods**

**By**

**Rolf Puchtinger**

**THESIS**

**Submitted to the Department of Geography  
in partial fulfilment of the requirements  
for the Master of Arts degree  
Wilfrid Laurier University  
1990**

**©Rolf Puchtinger, 1990**

## Abstract

Analyses of spatial point patterns tend to focus on deviations from randomness by either clustering or regularity. One assumption of these analyses implies that the point generating process is equal in all directions. However, the association of the location of points with a process biased in one or more directions is widely neglected due to a lack of appropriate statistical procedures. This is surprising, since patterns generated by directional processes are important in Geography. The purpose of this thesis is to investigate the blunt-triangle method and the third moment method for their potential of identifying directionality in spatial point patterns. A point process model is presented that combines the properties of both clustering and directionality. Realizations of this model are used with the objective of evaluating the two spatial analytical procedures. The blunt-triangle method is based on the comparison of blunt angles between triplets of points to theoretical blunt-triangle statistics. The failure of these statistics to find the characteristics given in the model can be explained by the dependence of the blunt-triangle method on assumptions of randomness. The third moment method examines the distributions of distances and angles between points, and is thus expected to be sensitive to a directional bias in spatial point patterns. It is shown that if the parameters of the procedure are chosen properly, different levels of directionality can be identified. The third moment method can thus be recommended for empirical applications in Geography.

## Acknowledgements

My thanks are due to the following people who helped this thesis become a reality. In particular, I would like to thank my advisor Dr. Barry Boots for initially suggesting this topic to me, and his encouragement through all stages of writing. Our discussions and his invaluable editorial comments helped me in finding the right direction and in making the points. I also would like to express my gratitude to Dr. D. Murdoch, Dr. H. Saunderson, and Dr. P. Kanaroglou for their insight and their helpful suggestions. Additional thanks go to the staff of WLU Computing Services; their help made the development and debugging of the program much easier. I am indebted and grateful to my parents for the support and encouragement they provided over the years. Last, but certainly not least, I want to thank my wife, Anne; her love, patience, and support always made it possible for me to keep writing.

## Table of Contents

Abstract .....	i
Acknowledgements .....	ii
List of Figures .....	v
List of Tables .....	viii
Chapter 1: Introduction .....	1
Introduction to the Topic .....	1
Objective of the Study .....	3
Outline of the Study .....	4
Chapter 2: Review of Existing Approaches .....	5
Methods of Point Pattern Analysis .....	5
The Method of Directional Statistics .....	8
Examples of Directional Point Patterns .....	10
Settlements (11); Sinkholes (16); Cirques (19); Drumlins (20)	
Chapter 3: The Methods .....	27
Finding Blunt Triangles .....	27
Conceptual Framework (27); Calculation of the Mean and the Variance of Blunt-triangles (30)	

Examination of the Third Moment Properties . . . . .	33
Chapter 4: A Model of the Directional Point Pattern . . . . .	39
Theoretical Considerations . . . . .	39
The Generation of Points . . . . .	44
The Introduction of Scale . . . . .	51
Chapter 5: Results . . . . .	56
Blunt Triangles . . . . .	56
Examination of the Tolerance Angle (56); Discussion (59)	
Third Moments . . . . .	64
Determination of Parameters (64); Findings (67); The	
Identification of a Second Direction (76)	
Chapter 6: Conclusions . . . . .	84
Summary . . . . .	84
Future Research . . . . .	87
Appendix . . . . .	89
References . . . . .	108

## List of Figures

Figure 2.1: Three general types of point patterns. . . . .	6
Figure 2.2: Distribution of settlements in a) Washington, b) Utah, c) Kansas, d) North Dakota. . . . .	12
Figure 2.3: Distribution of towns in Gippsland . . . . .	14
Figure 2.4: Distribution of dolines in south-west Germany. . . . .	18
Figure 2.5: Distribution of cirques in Tasmania. . . . .	20
Figure 2.6: Distribution of drumlins in Ireland. . . . .	21
Figure 2.7: Distribution of drumlins in Ontario. . . . .	23
Figure 3.1: Positions of 52 megalithic stones, Lands End, England. . . .	28
Figure 3.2: 81 blunt triangles with a $0.5^\circ$ tolerance from the megalithic stones. . . . .	29
Figure 3.3: Illustration of $S(\alpha; r_1, r_2)$ . . . . .	35
Figure 3.4: Positions of 62 redwood seedlings. . . . .	38
Figure 3.5: Short range and long range directional distributions of redwood seedlings. . . . .	38
Figure 4.1: Contours of equal density of bivariate normal distributions. . .	42
Figure 4.2: Algorithm for the directional point process. . . . .	43
Figure 4.3: 1 Cluster, 1 : 1. . . . .	46
Figure 4.4: 1 Cluster, 3 : 1. . . . .	46
Figure 4.5: 1 Cluster, 5 : 1. . . . .	46
Figure 4.6: 3 Clusters, 1 : 1. . . . .	47
Figure 4.7: 3 Clusters, 3 : 1. . . . .	47
Figure 4.8: 3 Clusters, 5 : 1. . . . .	47

Figure 4.9: 6 Clusters, 1 : 1. . . . .	48
Figure 4.10: 6 Clusters, 3 : 1. . . . .	48
Figure 4.11: 6 Clusters, 5 : 1. . . . .	48
Figure 4.12: 9 Clusters, 1 : 1. . . . .	49
Figure 4.13: 9 Clusters, 3 : 1. . . . .	49
Figure 4.14: 9 Clusters, 5 : 1. . . . .	49
Figure 4.15: 12 Clusters, 1 : 1. . . . .	50
Figure 4.16: 12 Clusters, 3 : 1. . . . .	50
Figure 4.17: 12 Clusters, 5 : 1. . . . .	50
Figure 4.18: 1 regional cluster, 2 local clusters. . . . .	54
Figure 4.19: 1 regional cluster, 4 local clusters. . . . .	54
Figure 4.20: 3 regional, 2 local clusters. . . . .	55
Figure 4.21: 3 regional, 4 local clusters. . . . .	55
Figure 4.22: 3 regional, 8 local clusters. . . . .	55
Figure 5.1: Acceptance areas for the null hypothesis of isotropy between +/- two standard deviations from the mean for a circular and a square convex hull. . . . .	57
Figure 5.2: Single Scale Model, 0 - Radius1, Sector Width=10°. . . . .	69
Figure 5.3: Single Scale Model, Radius1 - Radius2, Sector Width=10°. . . . .	69
Figure 5.4: Single Scale Model, 0 - Radius1, Sector Width = 12°. . . . .	71
Figure 5.5: Single Scale Model, Radius1 - Radius2, Sector Width = 12°. . . . .	71
Figure 5.6: Single Scale Model, Radius2 - Radius3, Sector Width = 12°. . . . .	71
Figure 5.7: Single Scale, 0 - R1, Width=15°. . . . .	74
Figure 5.8: Single Scale, R1-R2, Width=15°. . . . .	74

Figure 5.9: Single Scale, R2-R3, Width=15° . . . . .	74
Figure 5.10:Single Scale, R3-R4, Width=15° . . . . .	74
Figure 5.11:Double Scale, 0 - R1, Width=6° . . . . .	79
Figure 5.12: Double Scale, R1-R2, Width=6° . . . . .	79
Figure 5.13: Double Scale, R2-R3, Width=6° . . . . .	79
Figure 5.14: Double Scale, R3-R4, Width=6° . . . . .	79

## List of Tables

Table I: Constant terms of the second and third collinearity parameters for the corresponding convex hulls in the blunt triangle method . .	32
Table II: Standard deviations in the initial simulations, $\rho=0$ . . . . .	44
Table III: Standard deviations for the local-scale clusters. . . . .	51
Table IV: Percentages for the rejection of isotropy of the elliptical model. . . . .	59
Table V: Percentages for the rejection of isotropy for the rectangular model. . . . .	61
Table VI: Percentages for the rejection of the null hypothesis of isotropy for anisotropic point patterns on two levels of scale. Upper part: elliptical convex hull, lower part: rectangular convex hull. . . . .	63

## Chapter 1: Introduction

### Introduction to the Topic

The description and explanation of the spatial patterns of objects and events are two of the traditional intentions of geographic research (Harvey, 1968). The incidence of phenomena observed in the real world can be represented on a map by three basic geometric forms: points, lines, and areas. If the sizes of the objects are negligible when compared to the distances between them and the size of the study area, the objects can be represented as points (Hudson and Fowler, 1966). A spatial point pattern is then defined as a set of points distributed in a planar region. Thus, the statistical analysis of spatial point patterns allows the geographer to obtain a quantitative description of point pattern maps and in turn maps of different regions can be compared objectively. In addition, evidence can be gained to help identify the causal mechanisms that underlie the locations of objects in space.

Over the past decades a number of methods for the analysis of spatial point patterns have been developed that are now well established in geography as well as other disciplines. The approach common to most methods of *point*

*pattern analysis* is to examine how characteristics of a given point pattern relate to those of a pattern generated according to a specified process (Harvey, 1968). So far the characteristics of the point patterns examined in this way emphasize either the distances between points or the number of points in subareas. There has been little or no consideration of the orientation of the points with respect to each other or to the study area. This is surprising because such characteristics and the directional processes shaping them have long been important in Geography. One may think about major geomorphic processes: the movement of glaciers, the blowing of wind, and the flow of water; they clearly exhibit preferred directions. On the other hand, the flows of people, goods, services, and information are directional processes well known to shape the human landscape. Some of these processes, such as the wind direction, can be measured directly. Others that have vanished, eventually left features such as drumlins where directional measurements can be taken. In all cases, a set of angular data is obtained which can be examined using *directional statistics*. However, the procedures of directional statistics depend on frequency distributions derived from individual observations and do not consider the spatial characteristics of the pattern. Their usage in point pattern analysis is thus limited.

### Objective of the Study

From a review of present approaches (see Chapter 2) to both point pattern analysis and directional statistics it becomes apparent that until recently "... the detection of directionality is a virtually unexplored problem ..." (Ripley, 1979). However, the last years have seen the emergence in statistics of new theories and techniques, which might be appropriate to identify directional bias in spatial point patterns.

It is the purpose of this study to critically examine two recently developed techniques, the blunt-triangle and the third moment methods (described in Chapter 3), for their ability to detect directionality in spatial point patterns. This is accomplished by firstly developing an operational point process model that permits the extent of directional bias to be manipulated in several ways. The techniques are then examined to see how successful they are in recovering the extent of known directionality in the various realizations of the model. In other words, the methods are applied to simulated point patterns of known theoretical properties. The results of this procedure are used to make recommendations for applications to empirical geographical point patterns. In addition, helpful comments on the interpretation of the results of the methods are given.

### **Outline of the Study**

This chapter has identified the most commonly used approaches in point pattern analysis and in directional statistics; the objective of the study has been identified. Chapter Two will review the techniques and applications of point pattern analysis and directional statistics in geography and thus further justify the rationale of this thesis. The third chapter will introduce the two techniques to be examined. Chapter Four will present the directional point process model. The calibration of the techniques and the results of their examination will be outlined in Chapter Five. Finally, Chapter Six will summarize the study's findings and discuss the potential for further research in this area.

## Chapter 2: Review of Existing Approaches

### Methods of Point Pattern Analysis

The methods of point pattern analysis are comprehensively reviewed in the textbooks of Getis and Boots (1978), Cliff and Ord (1981), Ripley (1981), Diggle (1983), Upton and Fingleton (1985), and Boots and Getis (1988). Most methods of point pattern analysis proceed by comparing an actual pattern to a theoretical pattern generated from certain assumptions. The most basic hypothesis tested is that of *complete spatial randomness*, which arises from the *homogeneous, planar Poisson point process*. It is defined by the following two fundamental properties. Firstly, the number of points in a finite, bounded planar region with area  $A$  follows a Poisson distribution with mean  $\lambda A$ . In mathematical terms, the Poisson distribution can be written as

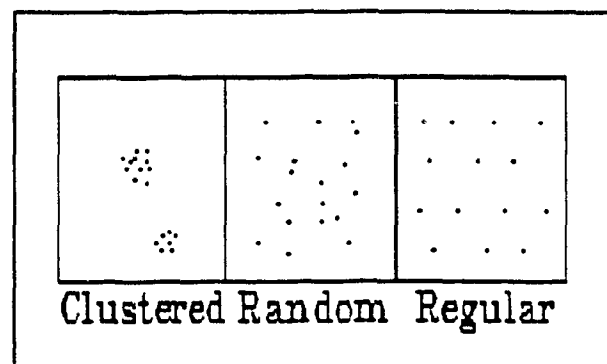
$$P(n; \lambda) = \frac{(\lambda A)^n e^{-\lambda A}}{n!} \quad \text{for } n=0, 1, 2, 3, \dots,$$

where the parameter  $\lambda$  is called the intensity of the process which is defined as the expected number of points per unit area, while  $n$  is considered a random variable representing the observed number of points in the region. The second property which can be defined as "purely random" or "completely random"

(Stoyan et al, 1987, p.42), is dependent upon the conditions of *uniformity and independence*. Uniformity implies that each location in the region has an equal probability of receiving a point. This means, that the study area can be regarded as homogeneous and being thus completely undifferentiated on the one hand, and that the point process is the same in all directions from every location regardless of the orientation of A on the other hand. The last quality is called *isotropy*, and the abstract geographical space of the homogeneous, planar Poisson point process is thus adequately termed the "isotropic plain" by Hägerstrand (1965). Finally, independence implies that the placement of one point does not influence the placement of any other point, which means that there is no interaction between points.

Obviously, patterns generated by a homogeneous, planar Poisson point process will hardly be observed in geographical reality. However, by relaxing the conditions of the properties of

**Figure 2.1:** Three general types of point patterns.



randomness the homogeneous, planar Poisson point process can serve as a starting point for models that approximate "geographical" point patterns more

closely. Thus, in addition to the random point patterns two other important general types of point patterns are frequently distinguished: *clustered* patterns and *regular* or *dispersed* patterns. Regular point patterns are thought to arise if the assumption of independence is violated in a way that the locations interact by repelling each other. This characteristic of repulsion may then indicate that some sort of competition or inhibition takes place. Clustered point patterns, on the other hand, can be explained by either environmental heterogeneity, which implies that some locations are more likely to receive a point than others, or that groups of points form because points attract each other. Consequently, more information about the study area is needed to decide whether the violation of the uniformity or the independence assumption has led to the agglomerations of points.

The most frequently used techniques to compare the properties of empirical point patterns to theoretical models can broadly be subdivided into two classes: *quadrat analysis* and *nearest neighbour analysis*. Quadrat analysis is applied by subdividing the study area into a number of subregions (quadrats) and counting the number of points in each quadrat. This information can be summarized as a frequency distribution which can then be compared to the expected frequency distribution of the hypothesized process. Nearest neighbour

analysis proceeds by comparing the characteristics of the distribution of distances between points and their nearest neighbours in the empirical point pattern with those expected in a theoretical point pattern. This method can also be extended to include neighbours of higher order. Other methods of point pattern analysis include second order methods, spatial tessellations, applications of information theory, trend surface analysis, and spectral analysis. However, it should be noted that neither do the given theoretical point processes incorporate directional characteristics, nor do the most frequently used techniques of point pattern analysis attempt to detect deviations from randomness by anisotropy. This implies that spatial analysts tend to accept the notion of an "isotropic plain" ignoring thus the influence of directions by assuming that the causal forces that locate phenomena in space are equal in all directions.

### **The Method of Directional Statistics**

The field of directional statistics arose from the need to find adequate methods of analyzing data that are distributed on a circle rather than having the nature of being on a linear level of measurement. An introduction to the methods of directional statistics with an emphasis on geographical examples is

given by Gaile and Burt (1980). The theoretical foundations of directional statistics are laid out by Mardia (1972). Batschelet (1981) provides a comprehensive overview about the techniques and the practical considerations implied. Usually, a directional analysis is initiated by taking individual directional measurements as orientations with a compass or a protractor. If the orientation of an undirected line is of interest, such as the strike of a fault line, the observations are called axes rather than directions. By assigning unit lengths to the orientations they obtain the property of magnitude and hence can be referred to as vectors. Now, the angular data can be regarded as being distributed on a circle of unit radius. By mathematical convention, a single observation represents the angle with the positive x-axis in counterclockwise direction. It should be noted that in this study angles are given in degrees if they refer to a conceptual idea, otherwise they are referred to in radians for computational purposes. Now, a variety of descriptive and inferential statistics can be applied. The former include the vector mean and the mean resultant vector length from which the circular variance can be derived. Inferential statistics of directional data include non-parametric tests as well as parametric ones, which indicate whether the data fits a circular uniform distribution or if it can be described by the von-Mises distribution. The latter is the circular equivalent of the linear Gaussian normal distribution, not to be confused with the

circular normal distribution used in Chapter 4. Thus, directional statistics are quite helpful in fields such as palaeocurrent analysis where a set of angular data can be obtained directly from sedimentary structures which is then used to infer the main direction of palaeocurrents. However, the appropriateness of directional statistics in point pattern analysis is quite questionable. Firstly, directional statistics are essentially non-spatial in the sense that no reference is made to the location of points or the distances between them. Secondly, there are no general rules agreed upon how to retrieve a set of vectors from a spatial point pattern.

### **Examples of Directional Point Patterns**

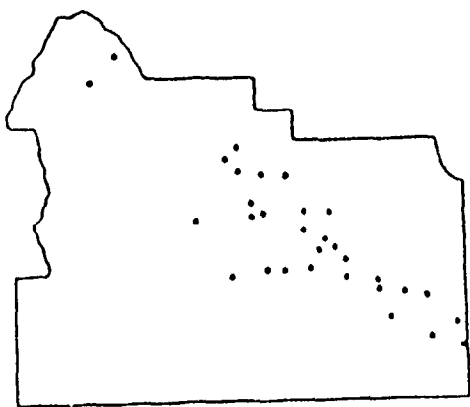
To illustrate the importance of the directional influence in point patterns some specific examples from both human and physical geography are examined. These are taken from the fields of the geography of settlements and from geomorphology. It should be kept in mind, that these point patterns are simplified representations of complex objects on the euclidean plane, where distances are straight lines. Consequently, additional information about neither topography and other environmental factors, nor the physical processes or human decisions that influence the location of geographic objects, can be expected to

be available.

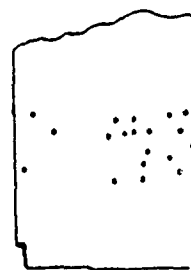
### Settlements

One of the interests of human geographers is directed toward the distribution of settlements across the landscape. With the help of the methods of point pattern analysis it is possible to objectively classify the distributions of settlements in different regions as more or less clustered, random, or regular. In addition, hypotheses concerning central place theory can be evaluated. In general, central place theory postulates that urban settlements form a hexagonal network on a featureless, isotropic planar surface that represents an optimal spatial equilibrium in a dispersed market situation with a uniform distribution of population, income, and consumer behaviour. In other words, settlements are expected to be regularly distributed according to the assumptions of central place theory. However, by analyzing the settlement patterns of twenty selected areas across the United States with a nearest neighbour technique, King (1962) finds all three general types of point patterns. One major factor identified to influence the actual locations of settlements is the development of a transportation network, in addition to variations in physical resources, the economic base, and land-occupance history. Thus, clustered patterns found in Washington and Utah (Figure 2.2 a and b) are attributed to the arrangement of towns along the major

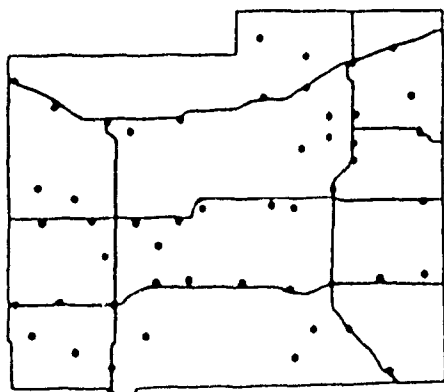
**Figure 2.2:** Distribution of settlements in a) Washington, b) Utah, c) Kansas, d) North Dakota. (Source: King, 1962)



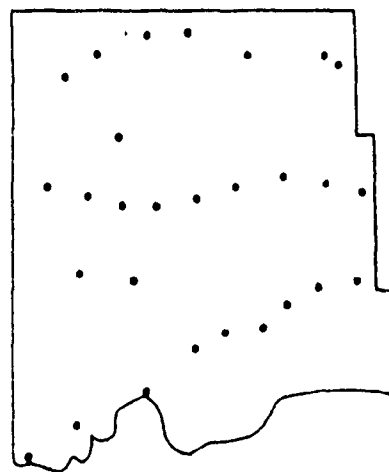
0 5 10 20  
Miles  
WASHINGTON



0 5 10 20  
Miles  
UTAH



0 5 10 20  
Miles  
KANSAS



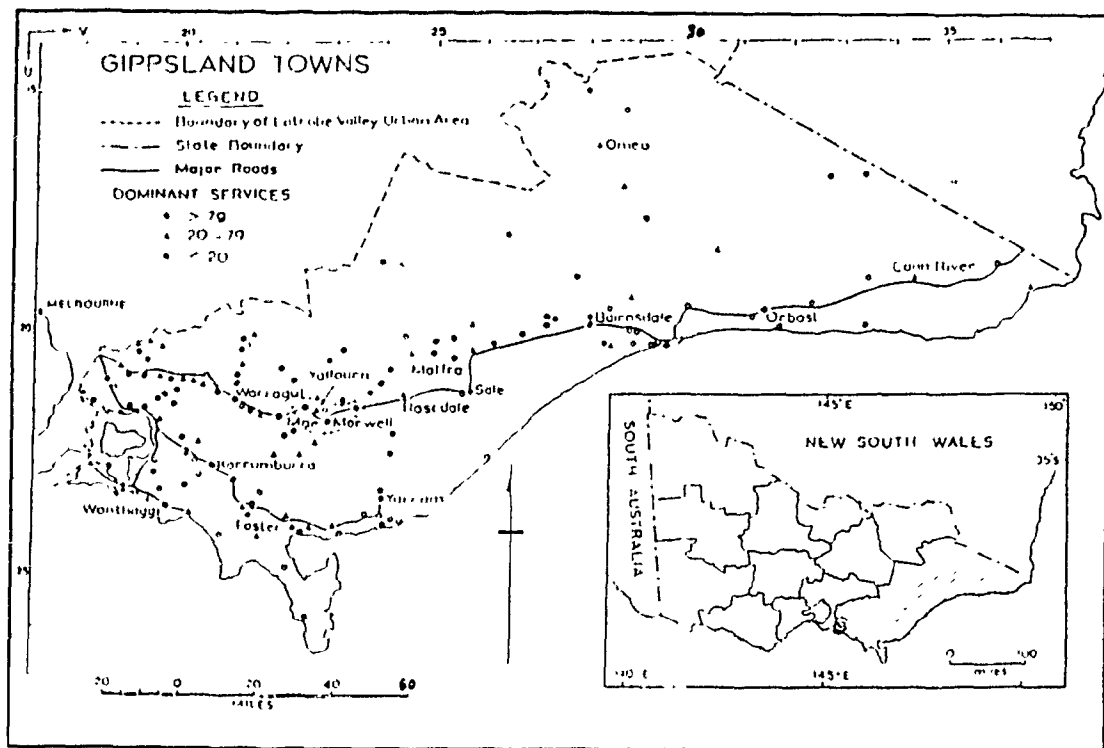
0 5 10 20  
Miles  
NORTH DAKOTA

rivers. Settlement patterns identified as being regular by nearest neighbour analysis are interpreted to be influenced by geomorphological features in Pennsylvania, where the settlements tend to be closely spaced in the northwest-southeast trending valleys, and by major transportation routes in Texas and Kansas (Figure 2.2c). The settlement pattern of North Dakota (Figure 2.2d), where settlements are basically located along three major transportation axes with an approximate east-west orientation, is identified by King as being random.

Clustering of settlements in Gippsland, a rural area in Australia, is shown by Norcliffe (1969) using a quadrat method. However, a visual inspection of the distribution of towns (Figure 2.3) suggests a close association of their location with the major roads which follow an east-west direction. Another example of clustered settlements is presented by Dacey (1968) who examined the distribution of houses in Puerto Rico. However, it is stated that the apparent clustering can not be completely explained by the given theoretical cluster process using a quadrat method. This may suggest that directional factors, which are unknown to the researcher, are influencing the clustering of houses in this example. A general explanation for the clustering of settlements is provided by central place theory by relaxing the assumption of a uniform population distribution. Now, settlements are expected to be clustered in sub-regions with

high population density. This leaves clustering as an alternative hypothesis which can readily be evaluated by the traditional means of point pattern analysis. Directional properties are introduced to central place theory by relaxing the assumption of isotropy. One approach includes the traffic principle which

**Figure 2.3:** Distribution of towns in Gippsland (Source: Robinson and Fairbairn, 1969)



implies the assumption that important towns are aligned on traffic routes. This results in an elongation of the hexagonal market areas along the routeways and an overall distortion of the regular pattern.

The interpretations of directionality mentioned above are based on geographical intuition rather than quantitative inquiry. More quantitative approaches toward the identification of a directional bias in settlement patterns are suggested by Hudson (1969) and Rayner and Golledge (1972). Hudson's (1969) pattern recognition approach consists of finding a type of pattern in search regions until the basic pattern changes. Rayner and Golledge (1972) applied spectral analysis to settlement patterns in Pennsylvania, North Dakota, and Oregon. In contrast to King (1962), they find the Pennsylvania settlements to be clustered, however they can confirm the southeast-northwest orientation quantitatively. A strong directional bias attributed to the development of transportation routes is identified in North Dakota and Oregon. In this respect it should be noted, that Gould (1967) clearly states that a well developed transportation network is likely to have only a weak orientation, whereas less developed transportation networks may exhibit a strong directional bias which becomes apparent in the distribution of settlements. This hypothesis is confirmed by Haynes and Enders (1975) and Upton (1986) upon the examination of settlement patterns in the time interval from 1914 to 1960 on a plain in Argentina. By using nearest neighbour methods regularity is detected in the 1914 pattern: however, a directional analysis of the angles between nearest neighbours reveals the directional bias which is focused on the source of

colonization. The 1960 pattern, however, shows new settlements that arose around the initial centres with a pattern tending more toward randomness or even clustering. Since the transportation network has now matured, the directional bias is no longer found between nearest neighbours. This shows, that a method with the ability of identifying directional properties of spatial point patterns would be most beneficial in cases, where little or no information about the transportation system is available such as some historical settlement patterns.

### Sinkholes

Interest in point pattern analysis is also displayed by geomorphologists concerned with the phenomenon of karst. Their attention is particularly focused on an explanation of the development and growth of the distribution of closed depressions in limestone areas. With this in mind, point pattern analysis has been used to examine whether subsurface solution and subsequent cavern roof collapse or near-surface corrosion can be identified as the process predominantly responsible for the distribution of sinkholes in a region.

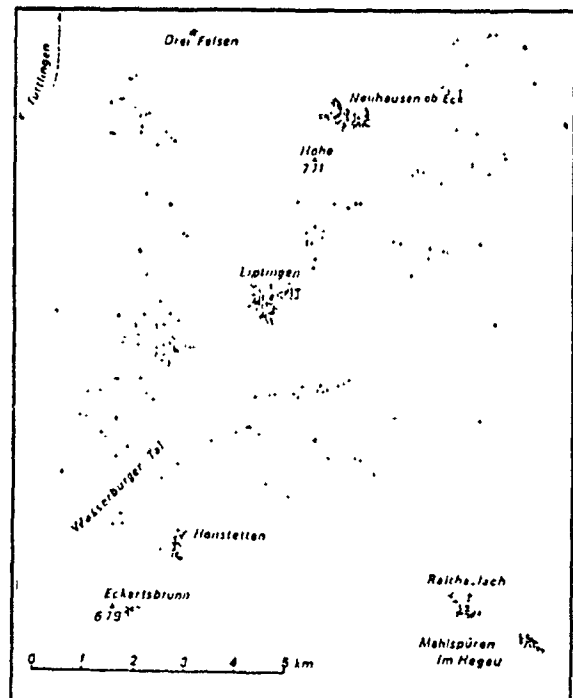
Using quadrat analysis McConnell and Horn (1972) found the distribution of karst depressions in Indiana being the reflection of two mutually independent random processes representative of the processes mentioned above. Ford and

Drake (1972) identified the clustered pattern of sinkholes in the Mendip Hills, England, to be the combination of two generations of features using both quadrat and nearest neighbour methods. This multigeneration theory is supported by Kemmerly (1982), who found a clustered distribution of 25000 depressions in Kentucky and Tennessee. Different conclusions are drawn by Williams (1971, 1972a, 1972b) and Day (1976). Williams(1971, 1972a, 1972b) applied nearest neighbour analysis to a number of cockpit karst areas in New Guinea finding them to be distributed between randomness and regularity. An interpretation of these distributions is that initial stream-sinks are either located at intersections of joints with a relatively regular joint system or that neighbouring depressions are in a state of balanced competition for space. A complimentary directional analysis of depression long-axes as well as the axes between nearest neighbours showed, that all karst features examined are to some extent aligned with features of geological structure. On a regional scale, the general slope corresponding to tectonic dip and master joints are identified as major directional factors. On the local scale the strike of the bedding plane assumes greater importance. Putting the evidence of point patterns analysis and directional examination together, Williams (1971, 1972a, 1972b) concludes that superficial chemical erosion is the major process in cockpit karst areas. His observations are confirmed by Vincent (1987), who analyzed the same data with a more refined nearest-neighbour

procedure which incorporates edge-effects. Similar observations to those in New Guinea are made by Day (1976) on karst features in Jamaica using identical techniques. Here, however, the possibility of subsurface solution and resulting collapse is not ruled out.

Other noteworthy attempts to prove the alignments of karst depressions with the associated geological structure are the pioneering studies of LaValle (1967) and Matschinski (1968). LaValle's (1967) approach includes estimating the percentages of solution depressions whose long axes are aligned with structural lineaments or with joint planes respectively. In addition, a

**Figure 2.4:** Distribution of dolines in south-west Germany. (Source: Matschinski, 1968)



mean elongation ratio is calculated. The approach of Matschinski (1968) bears some resemblance to the blunt-triangle method discussed in this thesis. He proceeds by finding the local orientations of aligned dolines in Germany (Figure 2.4). Maxima in the frequency distribution of the local orientations are

found to coincide with the adjoining regional structures rather than with the immediately underlying beds.

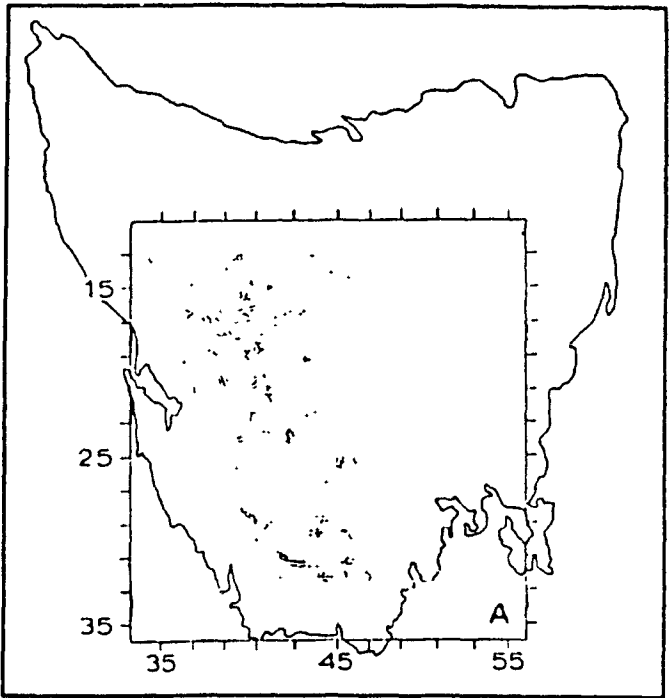
### Cirques

Geomorphologists and glaciologists are often interested in identifying the most important factors that control mountain glaciation. Among these factors are the pre-glacial relief, geological structure, glacial history, and the regional climate. One approach to infer the significance of these factors is by the study of the distribution and the orientation of cirques.

The distribution of cirques in Scotland is analyzed by means of quadrat analysis and nearest neighbour statistics by Robinson et al (1971). Robinson (1972) applied nearest neighbour statistics to the distribution of cirques in Tasmania (Figure 2.5). This method was also used by Unwin (1973) to examine the pattern of cirques in Wales, and by Trenhaile (1975) analyzing cirques in the Canadian Cordillera. All four studies find the distribution of cirques to be clustered, which indicates that the factors producing cirques favour certain parts of mountain ranges, which might themselves be clustered. However, Andrews and Dugdale (1971) show that the orientation of the cirque long axis is a more important variable for the explanation of glaciological conditions than the spatial

distribution of cirques. Thus, the analysis of the orientation of cirque long axes, which is dependent upon prevailing wind direction, general topography, exposure to sunlight, and bedrock structure (Vilborg, 1977) has been an integral part of several studies of cirque geomorphometry,

**Figure 2.5:** Distribution of cirques in Tasmania. (Source: Robinson, 1972)



including Andrews (1965), Sugden (1969), Andrews et al (1970), Evans (1972), Unwin (1973), King (1974), Trenhaile (1976), and Gordon (1977).

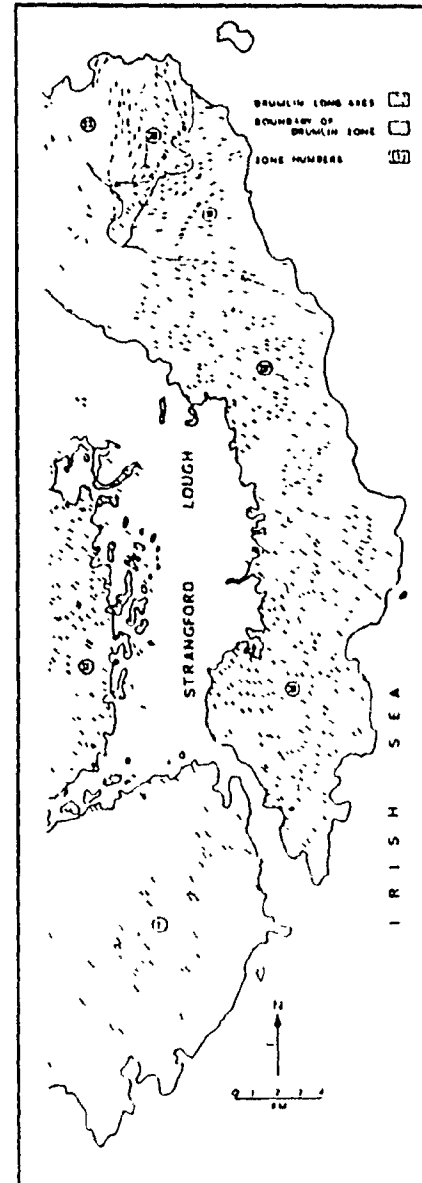
Drumlins

Some of the most remarkable signs of Pleistocene glaciation are the low, streamlined hills known as drumlins. Although geomorphologists have observed and examined drumlins for some time, no consistent theory has yet been derived to explain their origin and formation. However, the distribution of drumlins as well as their spacing and orientation are considered important variables for the

evaluation of hypotheses leading to a theory of drumlin formation, and for the comparison of drumlin fields.

An early attempt to quantitatively examine the origin of a drumlin distribution is the study of Vernon (1966), who observed an arrangement of drumlins in "...bands perpendicular to ice pressure with a weaker alignment parallel to ice flow..." in a drumlin field in Ireland (Figure 2.6). He substantiates this observation by contouring the density of drumlins and by calculating the mean distance between drumlins parallel and perpendicular to the flow of ice which is represented by the orientation of the drumlin long axes. Jauhiainen (1975) compared the distribution and orientation of drumlin fields in seven areas in north-eastern Europe. By applying nearest neighbour analysis he finds drumlins to be clustered in five areas and to be randomly distributed in two of the areas under

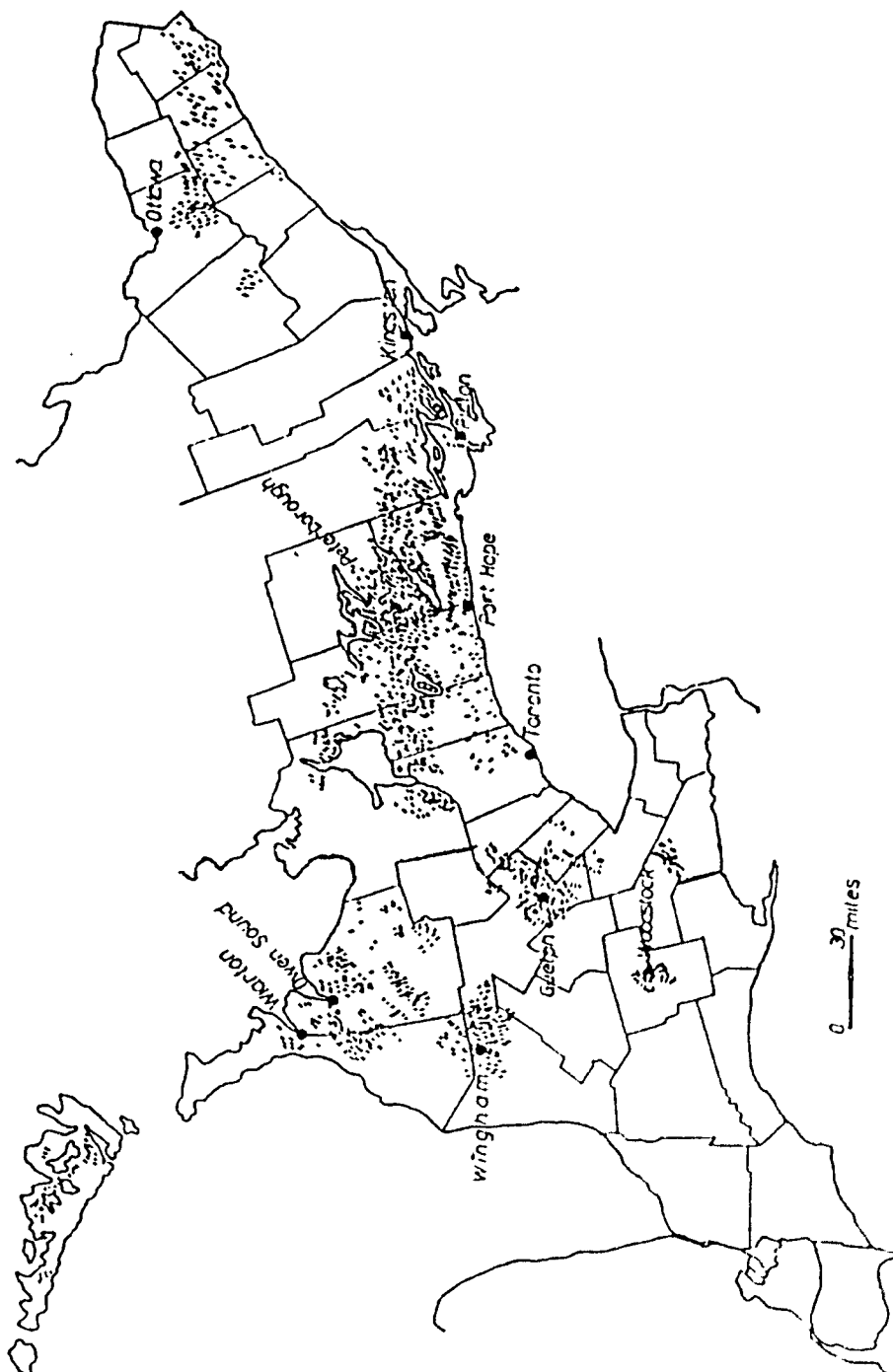
**Figure 2.6:** Distribution of drumlins in Ireland. (Source: Vernon, 1966)



investigation. With regard to the directional characteristics of the drumlins examined, it is found that the mean orientation differs in each of the study regions. A theory for the explanation of drumlin formation is examined by Smalley and Unwin (1968). This so-called dilatancy theory postulates that drumlins are the result of both erosional and depositional processes. The most important variable for the formation of drumlins is identified as the variation of properties in the available glacial till, which vary randomly. Thus, a non-random distribution of drumlins would not be expected. This hypothesis was in turn tested by Smalley and Unwin (1968) for drumlins in Ireland using nearest neighbour analysis, and with quadrat methods by Trenhaile (1971, 1975) for drumlin fields in Ontario (Figure 2.7), Gravenor (1974) for a drumlin field in Nova Scotia, and King (1974) for drumlin fields in England and New York. Their findings indicate that drumlins are distributed between randomness and regularity which suggests a confirmation of dilatancy theory. Additional analyses of the orientations of the drumlin long axes undertaken in the studies show normal distributions about a mean value, which indicates an even movement of the ice sheet while variations can be explained by local factors and short term changes in the direction of ice movement.

Although the results of the above researchers seem consistent and their

Figure 2.7: Distribution of drumlins in Ontario. (Source: Trenhaile, 1971)



conclusions logical, weaknesses and limitations with regard to the usage of point pattern analysis can be identified. These weaknesses are not limited to analyses of drumlin fields, they are equally valid for the examples of sinkholes and cirques mentioned earlier, since similar procedures of data acquisition and analysis are involved.

One problem particularly apparent in the point pattern analyses of drumlins mentioned above is identified by Hill (1973) as the neglect of patterns on different levels of scale. If for example the population of drumlins in Southern Ontario is inspected by eye, clusters of "drumlin fields" are obvious which can be associated with the "bands of drumlins" observed by Vernon (1966). Trenhaile (1971, 1975), however, follows the approach common among drumlin researchers to focus merely on the distribution of drumlins within distinct clusters rather than investigating the overall pattern or taking a random sample. With this in mind, Hill (1973) proceeded to analyze the distribution of drumlins in a large area in Ireland with a variety of point pattern techniques. He concludes that non-randomness can be observed on three levels of scale: on a regional level a decline in the density of drumlins from the centre towards the margins of the drumlin field is observed. A second scale of non-randomness consists of several alternating bands of high and low drumlin density perpendicular to ice movement. Finally a less strongly clustered pattern on a

local level is indicated.

Another problem inherent in the analysis of the distribution of sinkholes, cirques, drumlins, and other features stems from the reduction of a three dimensional object to a zero dimensional point (Boots and Burns, 1984). This creates artificial longer distances between the points resulting in an inhibition effect which biases the pattern towards regularity.

The third problem is associated with the precision of geomorphometric measurements. Frequently, measurements on geomorphic objects are taken from aerial photographs or from topographic maps rather than surveyed directly in the field. Rose and Letzer (1975) show that data derived from topographic maps with a scale as large as 1:25,000 are inaccurate when compared to direct field measurements and thus yield misleading results when further analyzed. These inaccuracies result from the accumulation of errors in the steps from the initial survey by non-geomorphologists over the interpolation of contourlines to the final measurements on the map. Problems of the accurate identification of geomorphic features are further increased by the fact that different researchers tend to define the variables that describe these features in different ways. For example Vilborg (1977) states that "...there does not seem to be any generally accepted definition of the orientation of cirques...".

With regard to the issues addressed in this thesis it becomes obvious from the geographical examples chosen, that apparent directional properties are neither picked up by quadrat methods nor by nearest neighbour methods which are the most popular point pattern techniques. It can also be seen that orientation measurements taken from individual geomorphic objects are hampered by problems of identification and definition and furthermore do not contribute to an understanding of directional characteristics between points and the study area. A noteworthy exception to merge point pattern analysis and directional statistics are the attempts to examine the orientations between nearest neighbours (Williams, 1971, 1972a, 1972b, Haynes and Enders, 1975, Day, 1976, Upton, 1986). However, by restricting the focus on directional properties between nearest neighbours, directional characteristics on a regional scale that might be present between neighbours of higher order are neglected. Thus, in a geographical context the above technique can not be recommended in general, while the need for more comprehensive approaches is obvious.

### **Chapter 3: The Methods**

It has been shown in the previous chapter that the most frequently used methods of point pattern analysis are unable to detect directional properties of spatial point patterns, and that the traditional techniques of directional statistics do not account for the spatial characteristics of the pattern. This chapter presents two methods to be examined later in this thesis, that are expected to pick up directional information in spatial point patterns and thus complement the traditional approaches of point pattern analysis. The first technique, here referred to as the blunt-triangle method, has been developed by D.G. Kendall and his co-workers at the University of Cambridge. Technique number two, here called the third moment method, has been suggested by J. Ohser and D. Stoyan from the Bergakademie Freiberg.

#### **Finding Blunt Triangles**

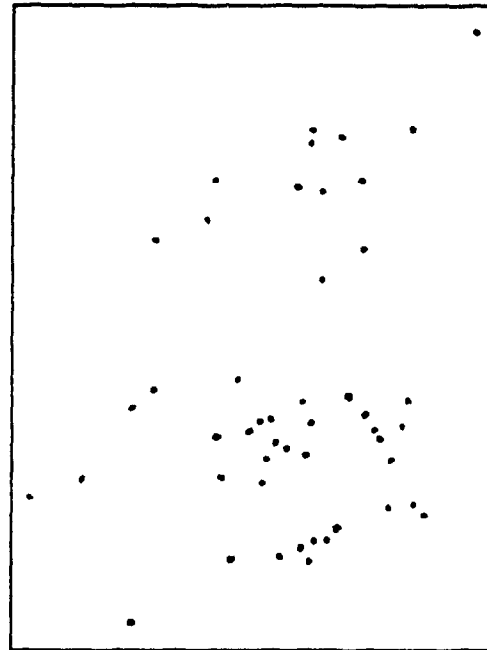
##### **Conceptual Framework**

The blunt-triangle method, also referred to as alignment method, was first applied by Broadbent (1980) to test whether 52 megalithic stones in Lands End, England, had been set out purposely to be aligned (see Figure 3.1). He proceeds

by forming  $\binom{n}{3}$  triangles out of  $n$  points. The next step involves the determination of the number of blunt triangles whose maximum angle is greater than or equal to  $\pi - \epsilon$ . The angle  $\epsilon$  is called tolerance, it is considered an unknown nuisance parameter which arises from the accumulation of errors by imprecisely setting up the stones, surveying them, and

finally reading their locations from a generalized map. With a tolerance angle of 30 minutes, 81 blunt triangles are found out of the total of 22100 triangles formed from the set of megalithic stones (see Figure 3.2). A method for the evaluation of  $\epsilon$  is developed by Kendall and Kendall (1980) which seems appropriate if one is concerned with alignments. According to the nature of the point patterns generated in the simulations and to the situation in

**Figure 3.1:** Positions of 52 megalithic stones, Lands End, England. (Source: Kendall, 1989)



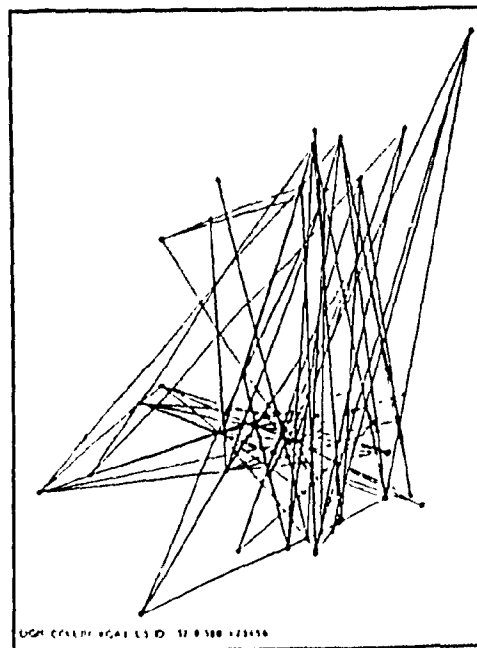
Geography, where point patterns evolve from rather complex processes, one would not expect points to be perfectly aligned by purpose. Instead, the term "blunt angle" can be perceived in broader terms rather than being limited to an approximation to collinearity. Hence, in the utilization of the blunt-triangle

method for the detection of anisotropy larger tolerances may be required and thus the estimation of  $\epsilon$  in this case is another subject of the study.

The number of observed blunt triangles can finally be compared to the expected number of blunt triangles and its

variance to test the hypothesis of alignment/anisotropy in the point pattern. In general, these values can be obtained by assuming that a point pattern has originated from a given probability distribution. If a known theoretical distribution is selected, the number of blunt triangles can be considered a random variable, and its mean and variance be either approximated by simulation or ideally be derived analytically. The development of the blunt-

**Figure 3.2:** 81 blunt triangles with a  $0.5^\circ$  tolerance from the megalithic stones. (Source: Kendall, 1989)



triangle method originated from a general framework which is known as the "statistics of shape" (Kendall 1984, 1989, Small 1988). In this framework a set of three points is defined as a shape which can be represented as a shape-point in the complex shape-space, if the effects of the rigid motions of euclidean

geometry, i.e. translations, rotations, and scalings, are removed. An examination of the distribution of shape-points projected on the unit sphere reveals properties of the shapes such as bluntness, that can not be easily recovered from the original distribution of points in the euclidean space. However, the mathematical concepts of this framework are rather involved and thus further discussion is well beyond the scope of this study.

#### Calculation of the Mean and the Variance of Blunt-triangles

In order to evaluate the general idea of the blunt-triangle method, a Poisson-cluster distribution or the Normal distribution would be appropriate models to calculate the mean and the variance of the number of collinear triangles, since these models are used to generate the point patterns used for examination of the methods in this thesis (see Chapter4). Unfortunately, the model of randomness had to be chosen, since explicit formulas for calculating the variance of the number of  $\epsilon$ -blunt triangles are only available for point patterns obeying the assumptions of independence and uniformity (Kendall and Kendall, 1980, Small, 1982). The calculation of the expected number and the variance for a number of  $\epsilon$ -blunt triangles ( $N(\epsilon)$ ) depends on the form of the convex hull of the point pattern. In the context of point pattern analysis, the convex hull is defined as the minimum convex set that contains a given set of

points. Here, it may be approximated by either a square, a rectangle, a circle, or an ellipse. Thus, it is important to consider the Broadbent-factor

$$\beta = (s + s^{-1})/2$$

for representing the stretch of the convex hull. The parameter  $s$  is estimated as the ratio of the principal component standard deviations, which are derived as the square roots of the two Eigenvalues from the variance-covariance matrix of the coordinates of the point pattern to be analyzed. For the case of the megalithic stones a value of  $s=1.661$  is derived which leads to a Broadbent-factor of about 1.1315. Now, the expected number of blunt triangles which are blunt at  $\epsilon$  radians can be obtained by

$$E(N(\epsilon)) = \beta \binom{n}{3} \eta \epsilon (1+e)$$

where  $\eta$  is called the first collinearity constant which is given by Kendall and Kendall (1980) as  $1/3$  for a square convex hull and  $1/\pi$  for a circular convex hull;  $e$  is an error term which is negligible for tolerances up to  $10^\circ$ . With given parameters, the expected number of blunt triangles for the megalithic stones is about 73 with a 30 minute tolerance angle. Considering a standard deviation of

about 12 (see formula below), the 81 blunt triangles found in the data set are not enough to reject the null hypothesis of no alignments. The formula for the variance is given as

$$\text{Var}(N(\epsilon)) = E(N(\epsilon))(1 - \beta\eta) + 3\binom{n}{3}\epsilon^2\left(\binom{n-3}{2}(\mu - (\eta\beta)^2) + \binom{n-3}{1}(v - (\eta\beta)^2)\right)$$

where  $\mu$  and  $v$  are the second and third collinearity parameters. Given the constant terms of Table I, the second and third collinearity parameters are defined by

	elliptical	rectangular
$\mu_2$	0.1103275111	0.1160346836
$\mu_0$	0.0075052729	0.0032940654
$v_2$	0.1801265487	0.1896296296
$v_0$	0.0600421829	0.0553058642

**Table I: Constant terms of the second and third collinearity parameters for the corresponding convex hulls in the blunt triangle method (after Kendall and Kendall, 1980).**

$$\mu = \beta^2\mu_2 - \mu_0 \text{ and } v = \beta^2v_2 - v_0.$$

It should be noted that the formulas and values given above are derived analytically under the assumption of randomness by Kendall and Kendall (1980). However, these assumptions are rarely if ever met in reality. In fact, the occurrence of clustering as one deviation from randomness is observed quite frequently in the selected examples and thus emphasized in the simulations of

this study.

To overcome the problem of clustering, Kendall and Kendall (1980) suggest a "randomization" procedure whereby the points are dislocated within a given distance. Broadbent (1980) indicates, that adding randomly simulated points to the observed ones, or subdividing the area into rectangular subregions with uniform point distributions might mitigate the problem. In the framework of this study, however, it seems more appropriate to examine the violations of the assumptions of uniformity and independence systematically with an emphasis on directionality and, hence, validate the adequacy of the blunt-triangle method for geographic point patterns.

### **Examination of the Third Moment Properties**

The second method to be tested in this thesis is an extension of the second moment measure, which is well established in point pattern analysis. It is based on the properties of a point process: The first moment measure  $\lambda$  is called the intensity of a point process, it is considered equivalent to the mean of a random variable and is usually defined as the number of points per unit area.

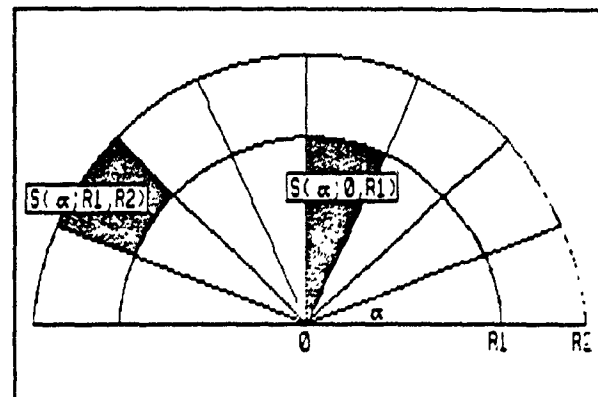
The reduced second moment measure  $K(r)$  is equivalent to the variance of a random variable and can be approximated by the distribution of distances between pairs of points (Ripley, 1976). Intuitively, the reduced second moment measure can be defined as  $\lambda^2 K(r)$  which is the expected number of ordered pairs of points within distance  $r$  of a point. Similarly,  $\lambda K(r)$  is defined as the number of further points within distance  $r$  of a random point.

In practical applications the expected value of the second moment measure can be calculated explicitly for a number of theoretical point processes where the underlying distribution function is known, including isotropic Poisson cluster processes (Diggle, 1983). With the help of simulations a confidence band can then be constructed from realizations of the theoretical point process (Ripley, 1977) and thus a test of statistical significance can be applied to the values of  $K(r)$  estimated from the data set of interest. The estimation procedure usually involves placing a disc of radius  $r$  on each point and summing up the number of pairs of points included in each disc. By increasing  $r$  from the smallest inter-point distance up to a maximum radius beyond which the results are biased, a cumulative frequency distribution of pairs of points can be established. However, since the point pattern is observed through a sampling window and therefore a subset of an unbounded, infinite population of points,

the point pattern will be continuous beyond its study area. Hence, if  $r$  exceeds the distance of a point to the boundary of the study area a part of the disc will be placed outside the study area and the estimation procedure described above will be biased. The problem of these so called edge-effects has been studied in depth by Ripley(1977, 1979, 1981, 1983, 1988), Ohser(1983), and Ohser and Stoyan(1981). Various modifications to the simplistic procedure outlined above are thus suggested by the development of estimators that not only account for edge-effects but also determine appropriate maximum values for  $r$ . However, it should be kept in mind that the derivation of the test statistics as well as the estimation of  $K(r)$  relies on the assumption of isotropy in the point pattern.

In order to use the **Figure 3.3: Illustration of  $S(\alpha; r_1, r_2)$ .**

properties of point processes for the detection of anisotropy, a reduced third moment measure  $K(S(\alpha; r_1, r_2))$  is introduced which examines the angular relationships



between two points (Hanisch, 1983, Ohser and Stoyan, 1981). In this expression  $S(\alpha; r_1, r_2)$  is defined as the intersection of a closed sector with midpoint on the origin and width  $\alpha$  with a disc if  $r_1=0$  and  $r_2>0$ , or an annulus if  $r_1>0$  and  $r_2>r_1$ .

$K(S(\alpha;r_1,r_2))$  is estimated as the number of points in the set  $S(\alpha;r_1,r_2)$ , by using each point in the point pattern as the origin. To use  $K(S(\alpha;r_1,r_2))$  for examination of a directional bias, the disc or annulus is subdivided into  $k=2\pi/\alpha$  sectors and  $K(S(\alpha;r_1,r_2))$  is estimated for each sector. Since an anisotropic bias is symmetrical, in all point patterns i.e.

$$K_i(S(\alpha;r_1,r_2)) = K_{i+k/2}(S(\alpha;r_1,r_2)) \text{ for } i=1,\dots,k$$

it is sufficient to consider the interval between  $0^\circ$  and  $180^\circ (= \pi \text{ radians})$  for examination and to use  $k=\pi/\alpha$ . The null hypothesis of isotropy can be evaluated by testing this distribution for uniformity. An appropriate significance test is a chi-square test of the form:

$$\chi_{k-1}^2 = \sum_{i=1}^k \frac{(K_i(S(\alpha;r_1,r_2)) - \frac{K(S(\pi;r_1,r_2))}{k})^2}{\frac{K(S(\pi;r_1,r_2))}{k}}$$

for  $0 \leq r_1 < r_2 < \infty$ ,  $i=1,\dots,\pi/\alpha$ . For graphical display as a (semicircular) histogram it seems preferable to plot the relative frequencies, which, according to Ohser and

Stoyan (1981), form a directional distribution

$$\theta_{r_1 r_2}(\alpha) = \frac{K(S(\alpha; r_1, r_2))}{K(S(\pi; r_1, r_2))}.$$

The modal class of this distribution as well as other major peaks in such a histogram are clearly indicative of preferred directions. Figure 3.5 shows the short range distribution  $\theta_{0,25}(10^\circ)$  and the long range directional distribution  $\theta_{25,50}(10^\circ)$  of a pattern of 62 redwood seedlings (see Figure 3.4). Both directional distributions indicate a main direction of about  $150^\circ$ . An obvious advantage of this approach, when compared to the blunt-triangle method or the second moment method, is its freedom from an underlying theoretical random model. Thus, it is not necessary for the researcher to firstly choose a known model and secondly go through the tedious process of fitting the chosen model to his data.

**Figure 3.4:** Positions of 62 redwood seedlings. (Source: Ohser and Stoyan, 1981)

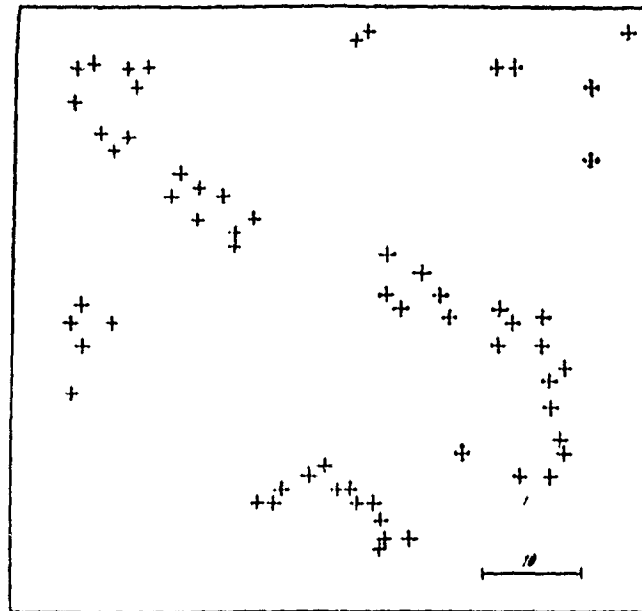
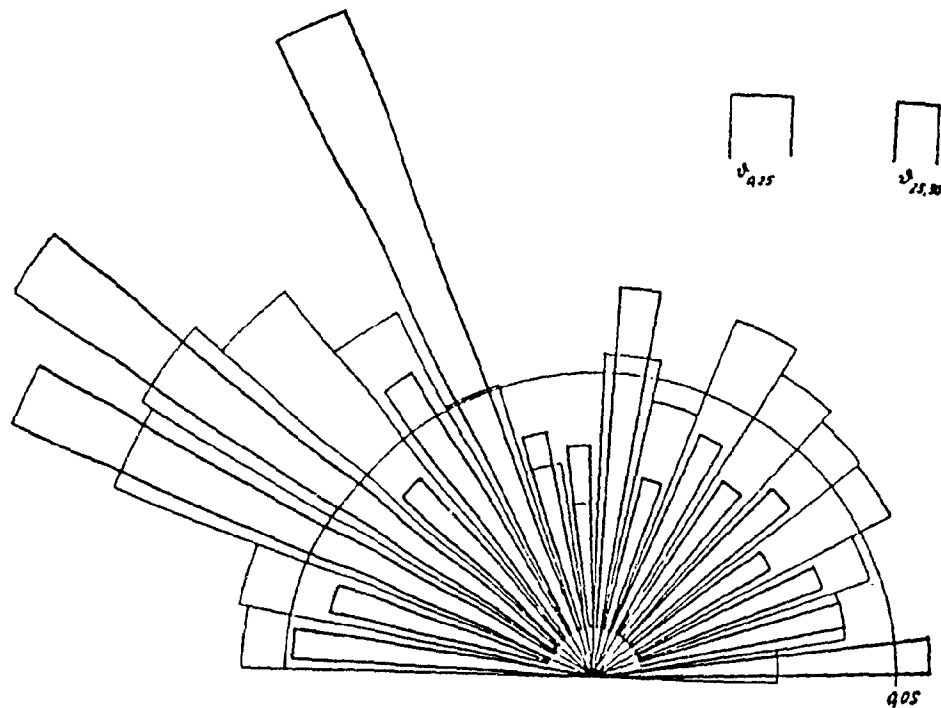


**Figure 3.5:** Short range and long range directional distributions of redwood seedlings. (Source: Ohser and Stoyan, 1981)



## **Chapter 4: A Model of the Directional Point Pattern**

### **Theoretical Considerations**

In the context of this study it can be seen in the selection of geographical examples, that the issue of directionality frequently occurs in conjunction with all three general types of point patterns. Often, however, directional point patterns can be directly associated with either visible or invisible linear features such as roads, fault lines, mountain ranges, or certain characteristics of glacier flow. The point patterns associated with these features then appear as bands or elongated clusters to the viewer. It is thus appropriate in a geographic framework to define a directional point pattern as a distribution of points around axes, with the density of points being a function of the distance of the points from the lines.

In order to construct a model of a point pattern suitable to assess the ability of methods to detect deviations from isotropy, the following two properties are to be considered. Firstly, the pattern has to be variable in the extent of clustering to account for the wide range of point patterns which can be encountered by the spatial analyst. Secondly, various levels of directionality

must be available to test the sensitivity of the methods.

The properties mentioned above can perfectly be met by the application of a particular Poisson cluster process, which can also be referred to as Neyman-Scott process. According to Diggle (1983, p.55), Poisson cluster processes can be generally defined by three postulates:

- "1. Parent events form a spatial Poisson process with intensity  $k$ .
2. Each parent produces a random number  $n$  of offspring, realized independently and identically for each parent according to a probability distribution  $\{P(n), n = 0, 1, \dots\}$ .
3. The positions of the offspring relative to their parents are independently and identically distributed according to a bivariate probability distribution. "

For the realization of point patterns in this study, the postulates above are slightly modified. Pertaining to postulate one, the numbers of parent events are externally fixed as  $k = 1, 3, 6, 9, 12$ , rather than sampled from a Poisson process for each simulation. Their locations are sampled from a rectangular random distribution. The number of offspring in a cluster is determined by a Poisson distribution with intensity  $\lambda = 60/k$ , thereby being conditional on the number of parent events. The overall intensity of points, 60, is chosen arbitrarily as a typical number of points occurring in empirical geographical point patterns.

Finally, the choice of the bivariate normal distribution allows the introduction of varying amounts of anisotropy into the point pattern.

The usefulness of the bivariate normal distribution as a generator of directional bias is emphasized by Hudson (1968) and Kendall (1984). Ohser and Stoyan (1981) exemplified an application of the third moment method using a Poisson cluster process with a bivariate normal distribution. Also known as elliptical normal distribution (Johnson and Kotz, 1972), the bivariate normal distribution is characterized by three parameters which determine its shape: the correlation coefficient  $\rho$  and the standard deviations  $\sigma_1, \sigma_2$  of the two variables respectively (see Figure 4.1). The ratio of the standard deviations determine the ellipticity of the distribution, and all three parameters define the angle of the major axis with the x-axis:

$$\Phi = \frac{1}{2} \arctan \left( \frac{2\rho\sigma_1\sigma_2}{\sigma_1^2 - \sigma_2^2} \right).$$

With a correlation coefficient of 0 and equal standard deviations the bivariate normal distribution is called circular normal, which is approximately isotropic. To account for different degrees of directionality, ratios of 1 : 1, 3 : 1, and 5 : 1 for the standard deviations appeared to be reasonable to distinguish between

**Figure 4.1:** Contours of equal density of bivariate normal distributions. (Source: Johnson and Kotz, 1972)

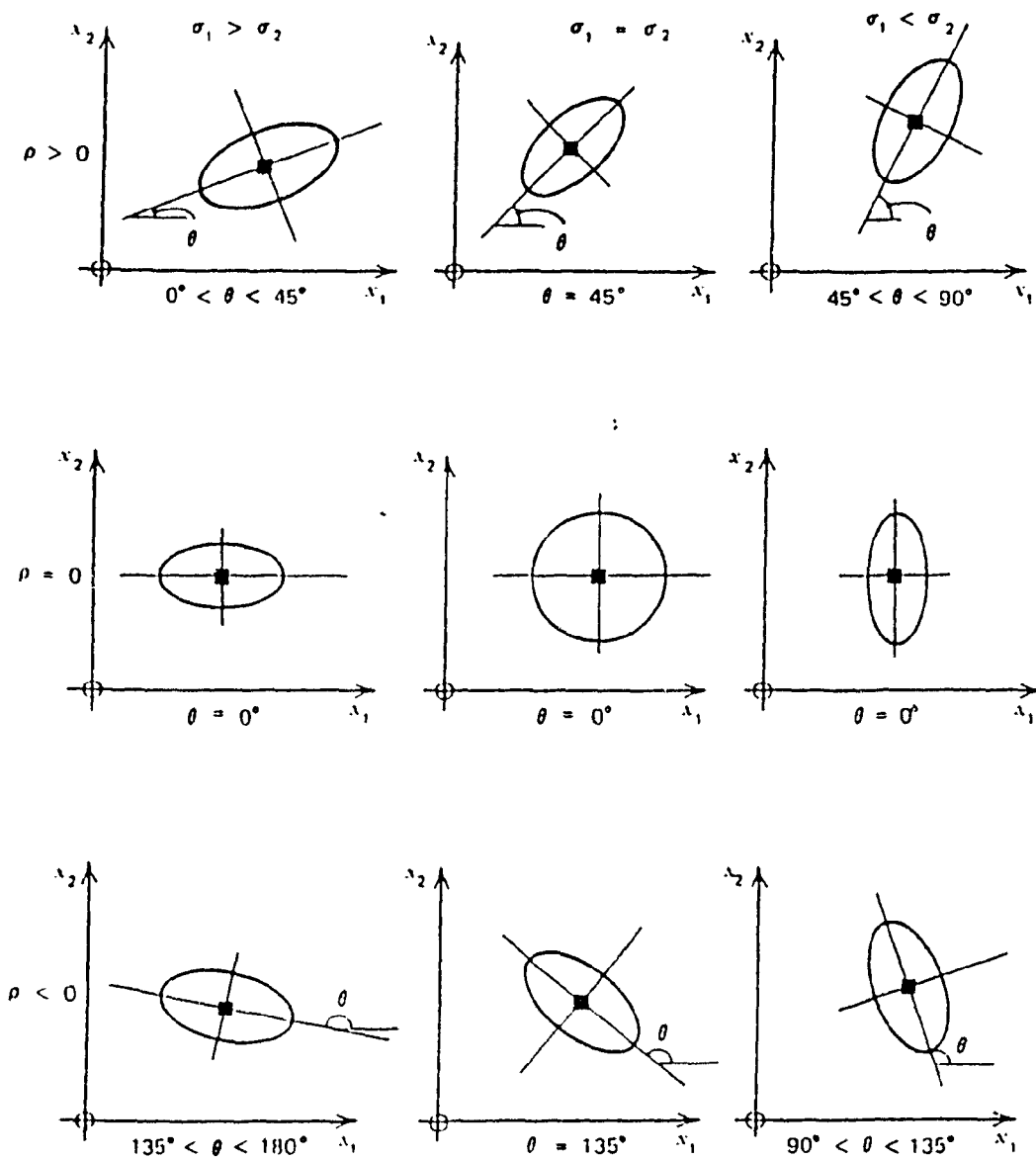
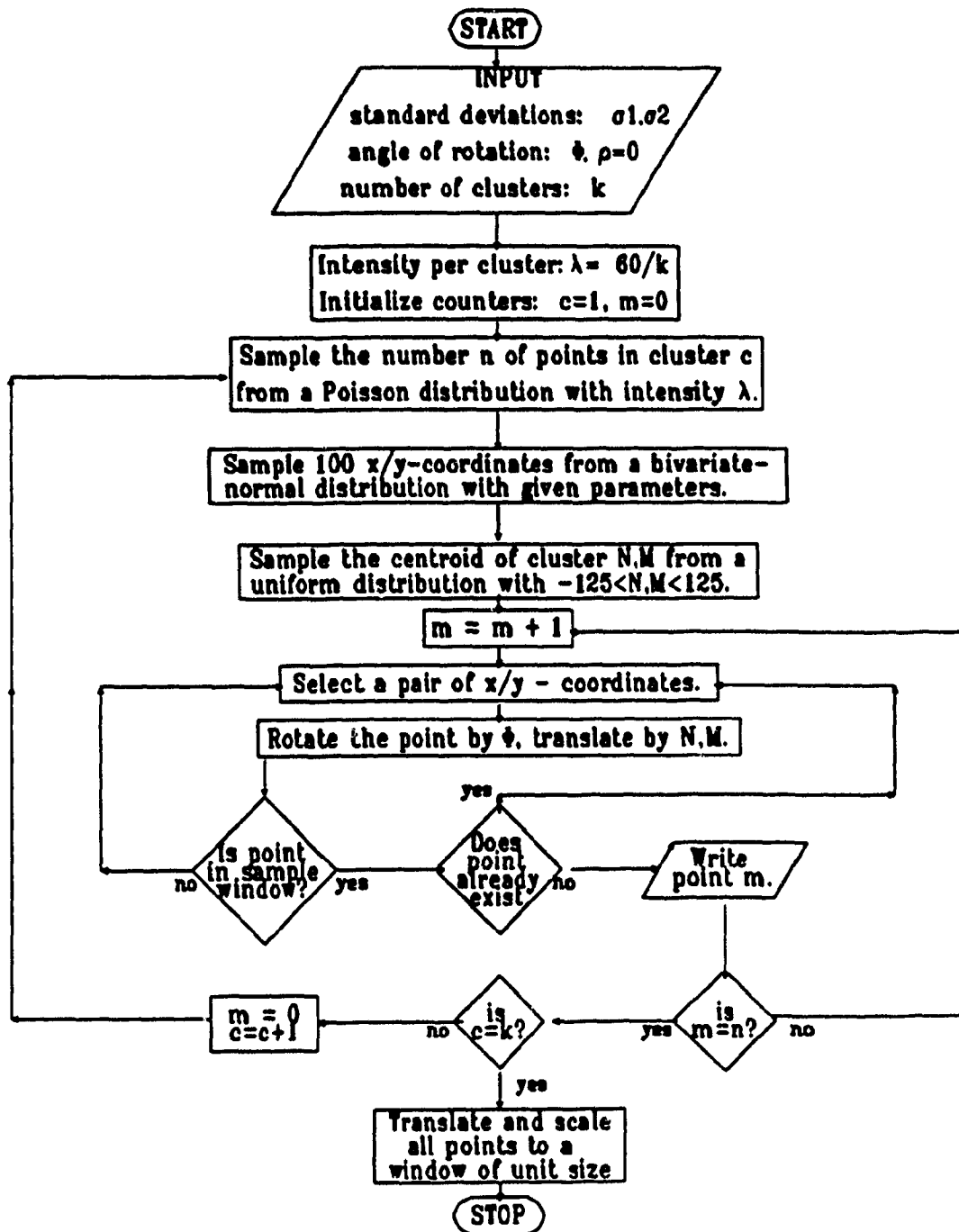


Figure 4.2: Algorithm for the directional point process.



isotropic, medium anisotropic, and strongly anisotropic point patterns respectively. The correlation coefficient is initially kept at 0.

**The Generation of Points**

CLUSTER	Number				
Ellipticity	1	3	6	9	12
1 : 1	120:120	100:100	80:80	60:60	40:40
3 : 1	108: 36	90: 30	69:23	48:16	30:10
5 : 1	100: 20	80: 16	60:12	40: 8	20: 5

**Table II:** Standard deviations in the initial simulations,  $\rho=0$ .

In practice the algorithm for simulating the particular Poisson cluster process proceeds as follows (see Figure 4.2). First, the coordinates of a cluster centre are sampled as random numbers in the range from -125 to +125 standard deviations. This range was chosen after a number of trial and error runs as being suitable to allow some overlapping of the large clusters on the one hand while on the other hand ensuring that even a large number of small clusters can be distinguished . Then, the number of points n for a cluster is generated by IMSL subroutine RNPOI, their locations determined by IMSL subroutine

RNMVN. In order to account for the variability of direction and thereby correlation, each point is subsequently rotated by an angle  $\Phi$  varying systematically for each simulation in a range from  $0^\circ$  to  $180^\circ$  in  $20^\circ$  increments, and translated by the coordinates of the cluster centre. Finally, a point is accepted for the point pattern under the conditions that its location is not yet occupied and that it is within a sampling window of size  $420 \times 420$  standard deviations. This larger final sampling window is necessary for maintaining the properties of clusters whose centres are placed close to the edge of the initial sampling range. Thus, artificially generated edge-effects which might cause biased results in the final outcomes are made negligibly small from the first. This procedure is repeated until the given number of uniformly distributed elliptical clusters is reached. To maintain  $\lambda$  as an overall intensity all points are finally rescaled to an area of unit size. Scatterplots of realizations of each of the directional scenarios summarized in Table II are provided in Figure 4.3 through Figure 4.17.

Figure 4.3: 1 Cluster, 1 : 1.

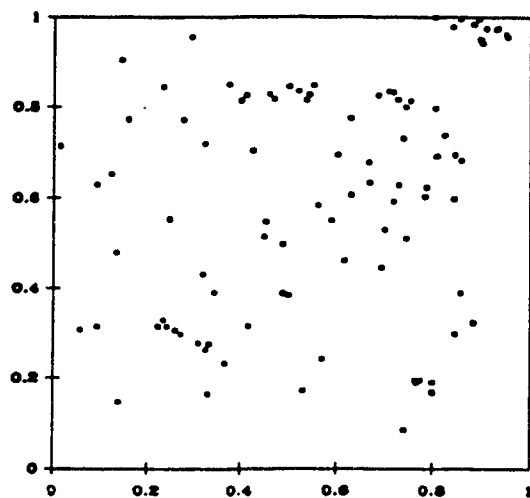


Figure 4.4: 1 Cluster, 3 : 1.

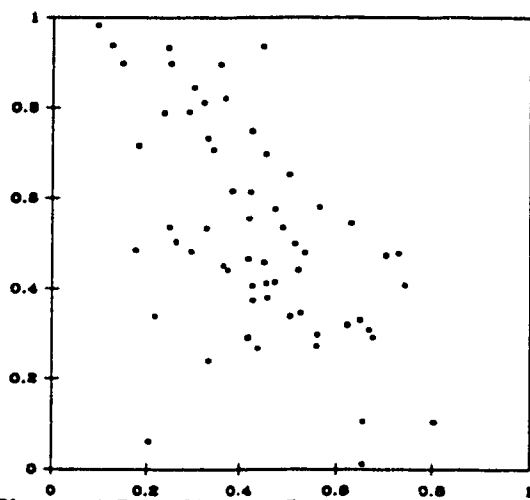
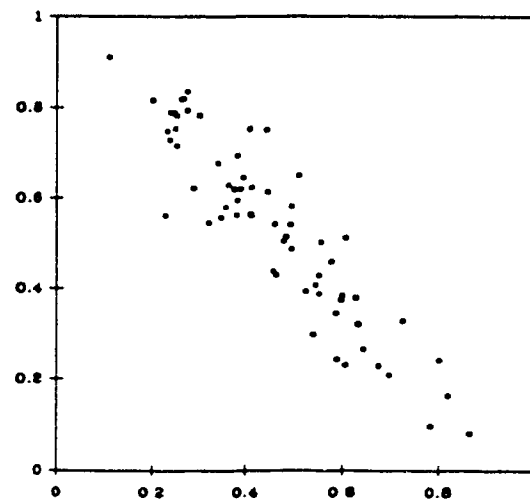
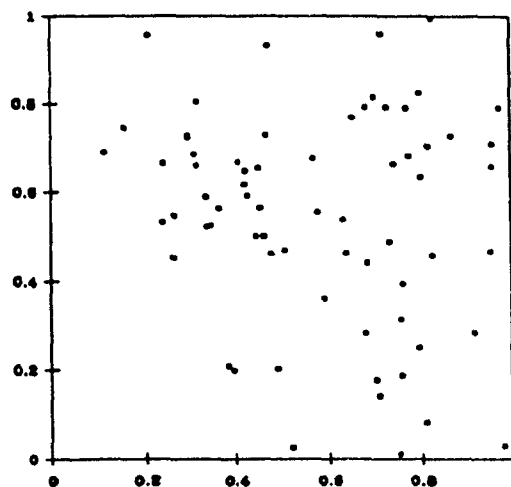
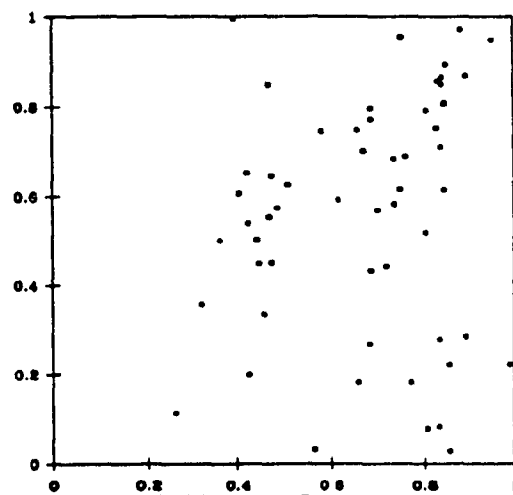
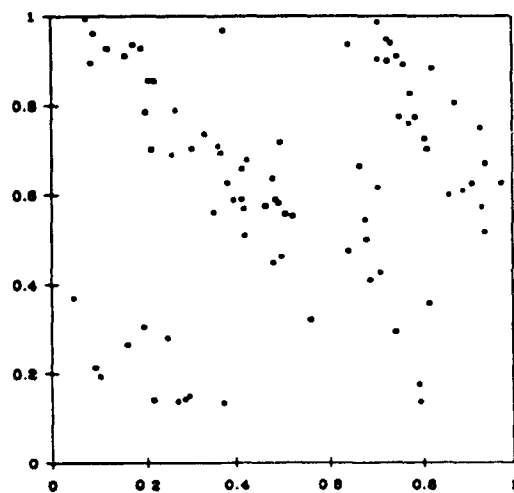


Figure 4.5: 1 Cluster, 5 : 1.



**Figure 4.6:** 3 Clusters, 1 : 1.**Figure 4.7:** 3 Clusters, 3 : 1.**Figure 4.8:** 3 Clusters, 5 : 1.

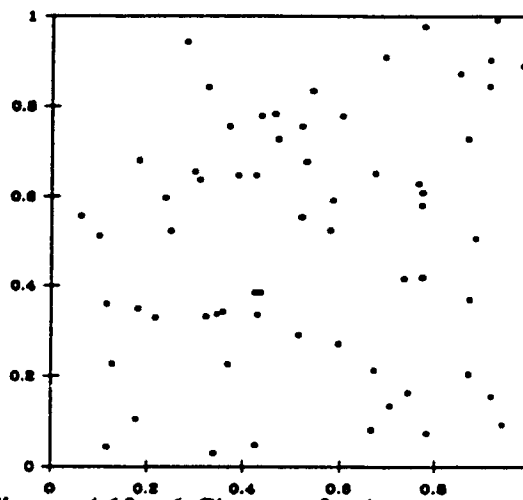
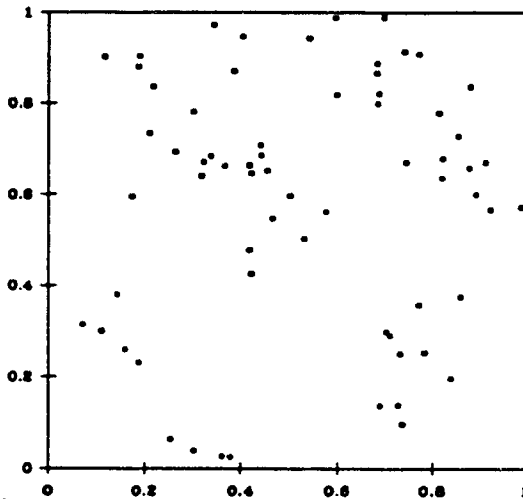
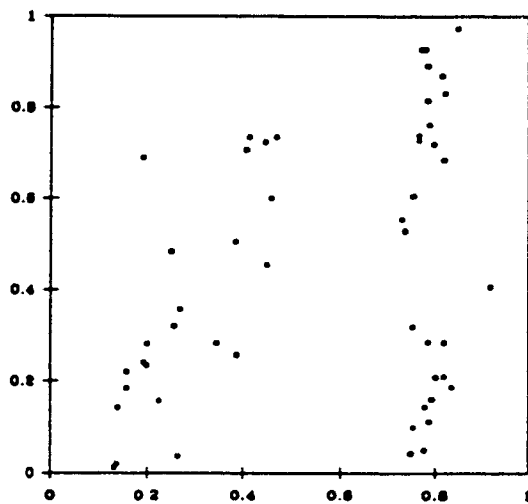
**Figure 4.9:** 6 Clusters, 1 : 1.**Figure 4.10:** 6 Clusters, 3 : 1.**Figure 4.11:** 6 Clusters, 5 : 1.

Figure 4.12: 9 Clusters, 1 : 1.

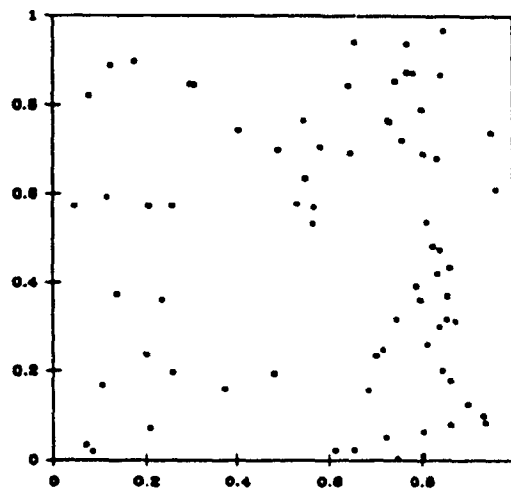


Figure 4.13: 9 Clusters, 3 : 1.

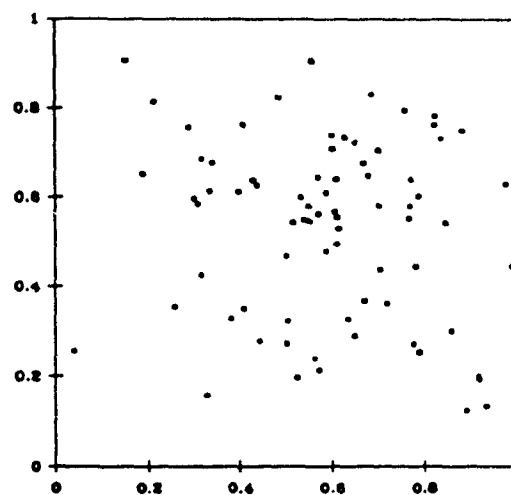
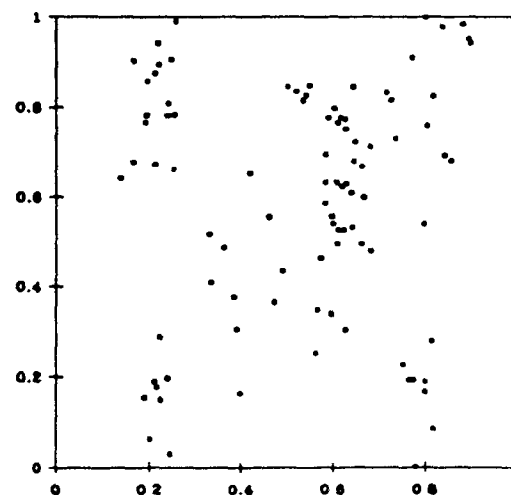
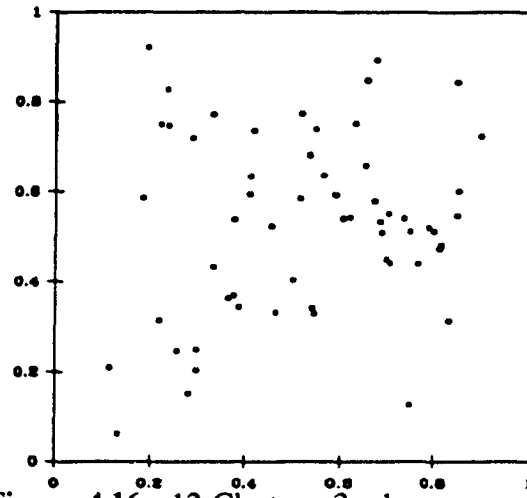
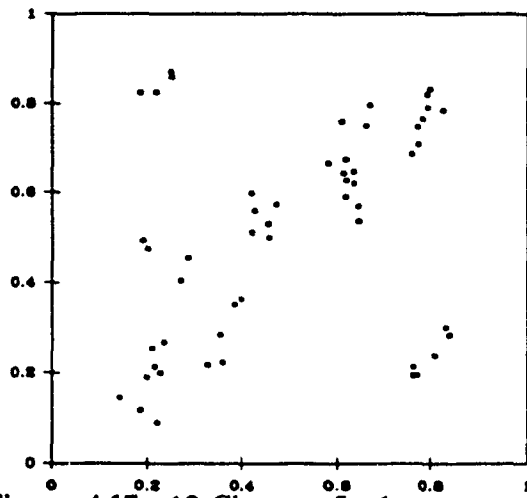
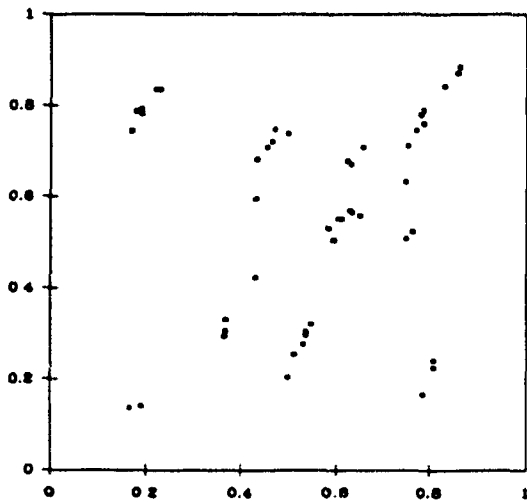


Figure 4.14: 9 Clusters, 5 : 1.



**Figure 4.15:** 12 Clusters, 1 : 3.**Figure 4.16:** 12 Clusters, 3 : 1.**Figure 4.17:** 12 Clusters, 5 : 1.

## The Introduction of Scale

Although quite complex directional point patterns can be generated under the assumption of being distributed about parallel axes, most geographers would agree that this assumption is too simplistic. In fact, at this point the model accounts for a directional process operating at the regional scale, such as the prevailing wind direction, the general flow direction of ice or water, or the direction of colonization in the examples chosen.

Hence, in order to make the model more realistic,

CLUSTERS	Local		
	2	4	8
1 (100:20)	60:12	45: 9	-----
3 (80:6)	35: 7	25: 5	20: 4

**Table III:** Standard deviations for the local-scale clusters.

directional forces operating on a local scale have to be considered as well. With respect to the examples these local directionalities are exemplified by local bedrock structure, locally varying glacier flow direction over time, or local links between the major transportation routes. In addition, a second level of scale not only represents local links between the major regional linear features in a spatial context, but also illustrates the evolution from a simple distribution to a more

complex distribution in a temporal manner.

Scale dependent complexity in the model can be accomplished by considering the sample to be drawn from the union of a "regional" set  $A_r$  generated by the procedure above and of a "local" set  $A_l$  generated in a similar fashion but with different parameters. The simulations of the point patterns evolve as successive generations of locations and follows this algorithm: First, a single-scale point pattern is generated according to the rules laid out in the sections above. Then, points are selected randomly as centres for the second-scale clusters, and, hence, serve as nodes of a network. The next step involves sampling of points from a bivariate normal distribution. These are in turn rotated by an angle orthogonal <sup>1</sup> to the direction of the primary point pattern, and translated to the selected node. An overall intensity of 100 was accomplished by adding the intensity of the local pattern, which was arbitrarily chosen to be 40, to the intensity of the regional pattern. Points on the regional scale were generated for the one and the three-cluster cases with the same standard deviations as outlined in Table II for the 5 : 1 ratio. These regional clusters were joined by 2 and 4, and 2,4 and 8 local clusters respectively (see Table III). Realizations of these point processes are shown in Figure 4.18 to Figure 4.22.

---

<sup>1</sup> An angle of 90° between the regional and the local direction is chosen for ease of distinguishing the appropriate modal classes in the third moment analysis.

With respect to geographical examples, one can now more easily associate a point pattern generated by this method with settlements or retail establishments distributed around the major roads in a transportation network. In physical geography, the association with the distribution of sinkholes or epicentres of earthquakes around fault lines would be appropriate.

In order to assess the power of the two methods the number of successful identifications of directionality out of a minimum of 100 simulations for each point process will be counted. Thus, the percentage of rejections of the null hypothesis of isotropy can be ascertained for each of the methods to be tested. In addition, the deviation of the direction predicted by the third order method from the given angle of rotation  $\Phi$  can be measured and an average directional deviation be established. This approach follows the method frequently applied for fitting models to real-life data sets (Boots and Getis, 1988, Ripley, 1977). In this manner, the two methods for the detection of directionality can be evaluated with regard to the potential to identify a major directional trend and its concentration. Furthermore, the ability to distinguish between regional and local directionality is also required so that the methods can be recommended for applications in Geography.

Figure 4.18: 1 regional cluster, 2 local clusters.

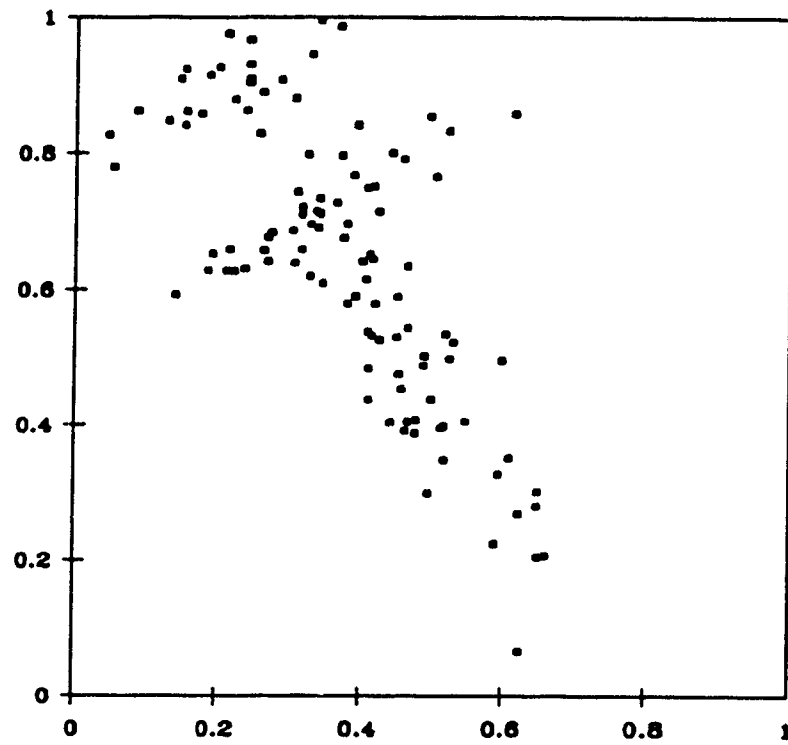


Figure 4.19: 1 regional cluster, 4 local clusters.

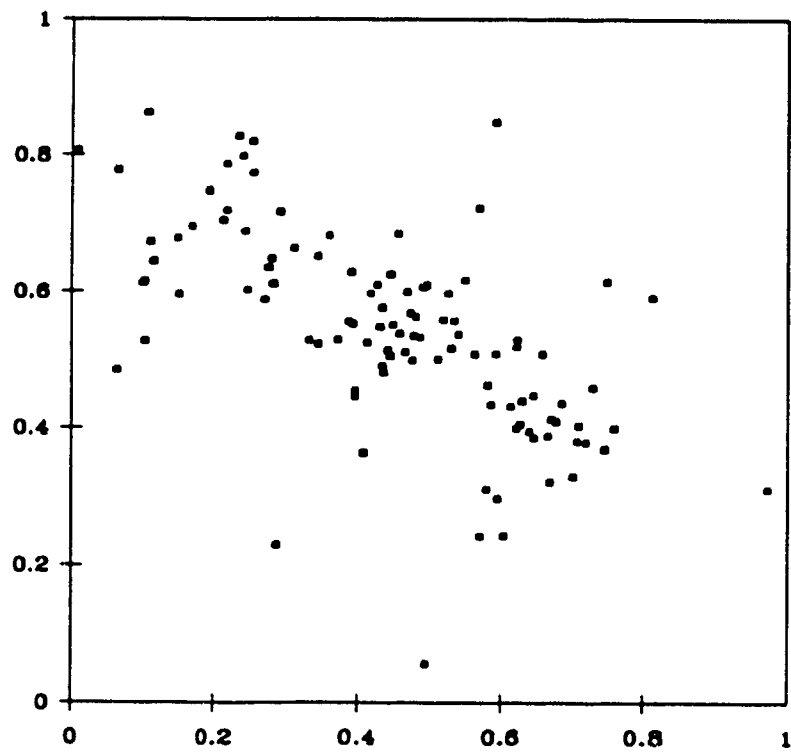


Figure 4.20: 3 regional, 2 local clusters.

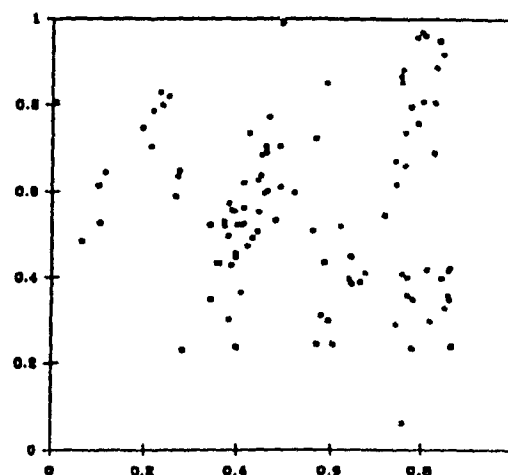


Figure 4.21: 3 regional, 4 local clusters.

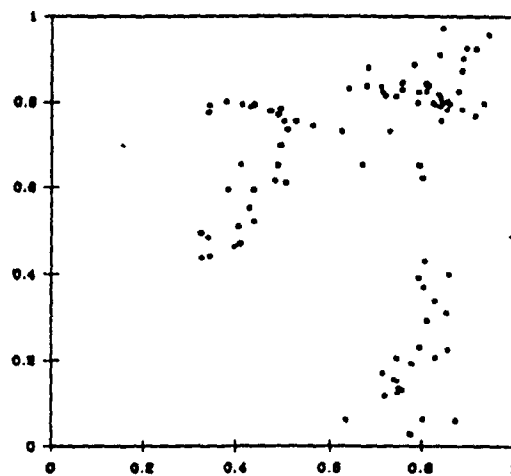
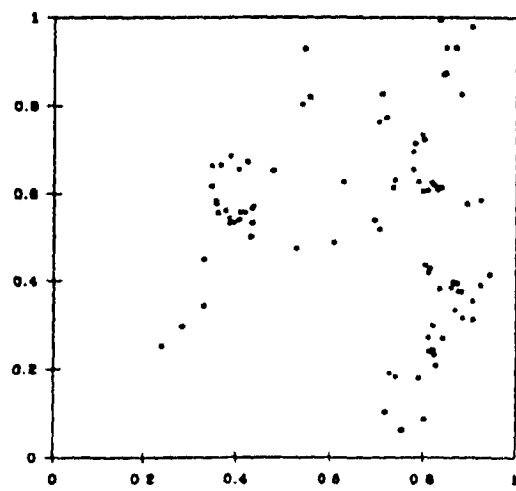


Figure 4.22: 3 regional, 8 local clusters.



## **Chapter 5: Results**

This chapter presents the results of the examination of the blunt-triangle method and the third moment method gained by their application to realizations of the directional point process introduced in the previous chapter. The results are preceded by sections illustrating the determination of parameters necessary to optimize the performance of the methods examined.

### **Blunt Triangles**

#### **Examination of the Tolerance Angle**

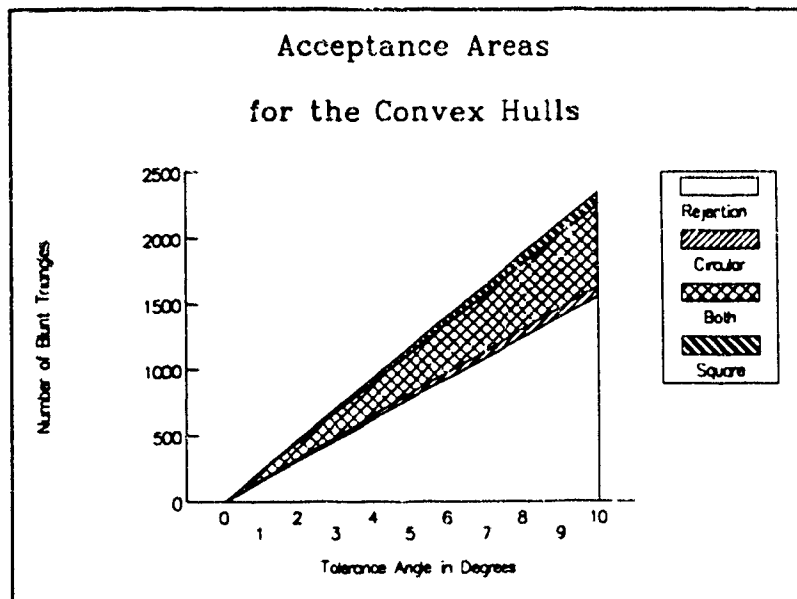
The first step in the evaluation of the blunt-triangle method is the examination of the behaviour of the tolerance angle in order to account for a broader definition of "bluntness" required for applications in Geography. Both Kendall and Kendall (1980) and Broadbent suggest choosing the tolerance angle as a small value ( $<1^\circ$ ). It is also clearly stated that the distribution of the largest angles are approximately uniform between  $170^\circ$  and  $180^\circ$  in a rectangular uniform point pattern (Broadbent, 1980), as well as in a Gaussian point pattern (Kendall and Kendall, 1980). This suggests examining the distribution of the

largest angles in the Poisson cluster process applied in this study for tolerances up to  $10^\circ$ .

Evaluating the tolerance was accomplished by increasing  $\epsilon$  in 6 minute increments from  $0^\circ$  to  $10^\circ$  and counting the number of triangles in the point pattern with an angle greater or equal

to  $\pi - \epsilon$ . The resulting cumulative frequency distributions appeared to be perfectly linear for all kinds of point patterns examined. Since the expected value and the variance for the uniformly distributed largest angles also increase linearly with the tolerance, it seems appropriate to consider the entire interval between  $170^\circ$  and  $180^\circ$  as a tolerance domain for tests of isotropy. Thus, instead of choosing arbitrary values for  $\epsilon$ , the slope of the cumulative frequency distribution for the largest angles can be computed for each empirical point pattern as well as the

**Figure 5.1:** Acceptance areas for the null hypothesis of isotropy between  $\pm$  two standard deviations from the mean for a circular and a square convex hull.



slope of the appropriate function of the standard deviations (the square root of the variance). On this basis, the null hypothesis of isotropy can be accepted with about 95% confidence, if the slope value for the cumulative distribution function (abbreviated: c.d.f) of the largest angles is within the range of the slope values of +/- two standard deviations about the expected number of blunt triangles. Figure 5.1 illustrates the linear behaviour of the parameters of the number of blunt triangles for random distributions of points in circular convex hulls and in square convex hulls with an increasing tolerance angle. For each of the convex hulls an area of 95% confidence of acceptance of the null hypothesis of isotropy is displayed as being filled. It is obvious that the acceptance areas for both convex hulls are largely overlapping, with the square acceptance area exceeding the circular one by about 10 blunt triangles per degree of tolerance. If the c.d.f. of blunt triangles of an empirical point pattern is plotted into this figure and its line is above an acceptance area, the null hypothesis could be rejected by reason of too many blunt triangles. On the other hand, the line of an empirical c.d.f. falling below an acceptance area could be interpreted as either "not enough" blunt triangles or, in other words, as an overprediction of the number of blunt triangles. It is not clear, however, how a point pattern with "not enough" blunt triangles could be defined or visualized.

Discussion

The results of the examinations of the blunt-triangle method over 500 simulations for each of the standard deviation ratios displayed in Table II are presented in Table IV for the collinearity parameters of an an elliptical convex hull, in Table V of a rectangular convex hull. Thus, the percentages in the rows from left to right correspond to an increasing number of clusters, while stronger directionality is represented down the columns.

Using the collinearity constants for an elliptical random distribution yields values for the rejection of the null hypothesis of isotropy from 10% to 45%. The highest rejection rates appear for the point patterns with a standard deviation ratio of 1:1. Hence, anisotropy is detected in over one third of 500 simulated point patterns, where no directionality is built in. In addition, the rejection rate

CLUSTER		Number				
Ellipticity	1	3	6	9	12	
1 : 1	42	38	38	40	32	
3 : 1	19	27	34	42	37 (1)	
5 : 1	10	33	41	43 (1)	45 (3)	

Numbers in brackets = overpredictions in percent.

**Table IV:** Percentages for the rejection of isotropy of the elliptical model.

drops sharply from a circular normal pattern to a highly directional pattern in the one-cluster case. For the cases of 3, 6, and 9 clusters the overall rate of rejection increases only slightly with the number of clusters. There is no evidence for a relationship between the increase of directionality and the rejection rate. Only for the case of 12 clusters, a coincidence is found between the increase of directionality and the rejection of isotropy. Nevertheless, ideally one would expect the percentage to range from about 5% for the circular normal pattern to about 95% for the anisotropic pattern. The range from 32% to 45% is thus unsatisfactory for a method supposed to be able to detect directionality. It should also be noted that the null hypothesis is rejected for 3% of the highly anisotropic 12-cluster patterns because "not enough" blunt triangles are found. This fact further weakens the acceptance of the blunt-triangle method for applications with clustered point patterns.

Table V presents the results for the blunt-triangle method using collinearity constants of the rectangular model and shows slightly better, but still unsatisfactory results. The rejection rates of 12% to 16% for the non-directional patterns indicate improved performance of the rectangular approach when compared to the elliptical approach. The rate of rejection of the null hypotheses generally increases with the number of clusters in the directional point patterns.

Less directionality is found by the blunt-triangle method in the more directional 1 and 3 cluster patterns. For the 6, 9, and 12 cluster cases the predictions follow the built-in directional properties. Similar to the elliptical model, an increasing percentage of rejections is generated by overpredicting blunt triangles for cases with high clustering and high directional bias.

CLUSTER	Number				
Ellipticity	1	3	6	9	12
1 : 1	13	12	15	15	16
3 : 1	13	15	22	26(1)	28(2)
5 : 1	9	12	30(1)	37(3)	40(6)

Numbers in brackets = overpredictions in %.

**Table V:** Percentages for the rejection of isotropy for the rectangular model.

The obvious failure of the blunt-triangle method for the one-cluster case can clearly be attributed to the use of different models for the generation of geographic point patterns on the one hand, and the derivation of the test statistics on the other hand. In particular, one could assume that the non-uniformity of point distributions evolving from the circular normal generator might bias the outcome of the evaluations. It seemed therefore reasonable to supplement the

previous analyses with a subsequent evaluation of the blunt-triangle method applied to approximately random point patterns. The additional applications of the blunt-triangle method to 100 patterns of 60 points distributed by the IMSL random number generator in a 250\*250 rectangle yielded 7% of rejections with the use of an elliptical convex hull, and 3% of rejections for the statistics under the assumption of a rectangular convex hull. These acceptable results confirm, that particularly in the one-cluster case the changing density of points from the centre to the edge of the cluster influences the number of blunt triangles in a manner unforeseeable by the test statistic.

Finally, the results of 400 applications of the blunt-triangle method to simulated point patterns with directionality induced on two levels of scale are summarized in Table VI. For either of the rectangular or the elliptical model the rejection rates decrease when further local clusters are added. As for the influence of the number of regional clusters, the highly directional point patterns with one regional cluster yield reasonable results in the range of 87% to 97%. However, the drop to a range of 32% to 48% for highly directional point patterns with three regional clusters, with up to 5% rejections induced by overpredictions, is clearly beyond acceptability. It should be noted, that these results coincide with the percentages attained for the monodirectional point

patterns with six or more clusters.

All in all, the blunt-triangle method performs poorly in most of the cases considered. For non-directional patterns, the null hypothesis is generally rejected far too often. Not even 50% of rejections are reached for highly directional point patterns. Exceptions,

where the blunt-triangle method shows an acceptable behaviour are limited to random point patterns and highly directional point patterns with one regional cluster and some local clusters with an orthogonal orientation. In all other cases

CLUSTERS		Local		
Regional	2	4	8	
1	97	91	-----	
3	48(2)	42(1)	40(1)	
1	95	87	-----	
3	42(5)	35(5)	32(4)	

Numbers in brackets=overpredictions in %.

**Table VI:** Percentages for the rejection of the null hypothesis of isotropy for anisotropic point patterns on two levels of scale. Upper part: elliptical convex hull, lower part: rectangular convex hull.

where the blunt-triangle method was evaluated not enough coincidence was found between the properties built into the patterns and the outcome of the analyses. It can thus be concluded that the blunt-triangle method with the application of collinearity constants for elliptical and rectangular random models is unsuited for Poisson cluster processes. Since it is likely that Poisson cluster

processes represent a larger subset of point patterns observed in geographic reality than homogeneous random processes do, it is hoped, that blunt triangle statistics based on Poisson cluster processes will be available sometime in the future.

### **Third Moments**

#### **Determination of Parameters**

The first issue arising in the application of the third moment measure is the choice of appropriate values for the angle of a sector as well as the radii. If one is interested in second moments, the use of all inter-point distances as radii is an elegant way to handle the latter problem (Boots and Getis, 1988). However, in the examination of anisotropy the choice of particular distance intervals is beneficial since this leads to a way to observe variations of directionality on different levels of scale. In addition, it will be seen later how variations in the density of points in different annuli are helpful in the identification of clustering and in the determination of the size of the clusters.

The choice of the sector size, on the other hand, determines the proper

identification of the orientation of the directional bias. If the sector size is too small a significant mode will be hard to identify, with increasing class width less precise directional information will be given. An additional constraint on minimizing the annulus and the sector sizes is the requirement of the chi-square test, that the expected value of the distribution to be tested (here:  $K(S(\pi; r_1, r_2))/k$ ) should not be less than 5. With this in mind, it seemed appropriate to run a number of trial and error analyses in order to calibrate the parameters.

For the radii, the initial configuration was the maximum inter-point distance subdivided into equidistant intervals as annuli. It became obvious that the outer annulus as well as the inner disc did not receive enough points to qualify for the chi-square test. Thus, several improvements became necessary. Firstly, the maximum radius had to be limited to avoid biased results. Most researchers using the second moment method define the maximum radius as a value which depends upon the size of the study area. In particular, the circumradius (Boots and Getis, 1988) and the diameter (Ohser, 1983) of the study area are values chosen frequently in accordance with the estimation procedure. In the context of this thesis, however, it was felt that considering the process generating the point patterns a maximum radius dependent only on the relative locations of points would be more appropriate. One solution is to

choose the convex hull of the point pattern as an unequivocal "natural" border, and deriving the circumradius from the eigenvalues computed previously for the blunt angle method as:

$$r_{\max} = \sqrt{E_1 + E_2}$$

where  $E_1$  and  $E_2$  denote the first and the second eigenvalue respectively. Another improvement was accomplished by subdividing the maximum disc into annuli of equal area, making thus the different  $K(S(\pi;r_1,r_2))$  proportional to relative densities of points in the annuli.

With respect to the class width, initial values of  $2^\circ$  were chosen as sector angles. However, this high degree of precision is not needed since for the more clustered patterns misclassifications from the given direction of up to a magnitude of 15 classes were observed. Hence, a maximum class width of  $15^\circ$  is still considered appropriate for maximizing the probability of the modal class to receive the "correct" direction.

Finally, the following experimental designs were set up to each carry out 100 analyses for the standard deviation ratios shown in Table II. The first set up implied the subdivision of the maximum radius into a disc and an annulus of equal area, and a sectoral angle of  $10^\circ$ . Thus,  $K(S(10^\circ;0,R_1))$  and

$K(S(10^\circ; R_1, R_2))$  were to be estimated in the first experiment with radii calculated as:

$$R_2 = r_{\max} , \quad R_1 = \sqrt{\frac{R_2^2}{2}} .$$

Experimental set ups two and three were defined by an increase to three and four distance intervals, and sectoral angles of  $12^\circ$  and  $15^\circ$  respectively. In each experiment the  $K(S(\alpha; r_1, r_2))$  were estimated and absolute frequency distributions as well as a chi-square value for each distance interval were obtained. Then the chi-square value was compared to an appropriate tabulated value to test the null hypothesis. If the null hypothesis was rejected the modal class was determined and its deviation from the given angle of rotation  $\Phi$  measured. This procedure repeatedly carried out over 100 simulations for each standard deviation ratio thus yielded accumulated percentages of the rejections on the 0.05 significance level and additional average misclassifications for each of the distance intervals.

### Findings

Figure 5.2 to Figure 5.10 illustrate the results for the application of the third moment method to the point patterns generated with the standard deviations from Table II. The vertical axis in each figure displays the total number of

simulations as 100%. Each bar in the figures thus portrays the percentage of rejections of the null hypothesis of isotropy on the 0.05 significance level, in addition to the percentage of cases where the minimum number of expected class frequencies is less than 5 and thus, the assumption of the chi-square test is violated. On top of each bar the average misclassification, based on the class width in the directional distribution, of the detected modal class to the given direction is displayed. The horizontal axis shows the character of the simulations with the number of clusters in ascending order. To each number of clusters there are assigned three bars according to the strength of directional bias. The first bar in each group is representative of an isotropic pattern (1:1 standard deviation ratio) where no directionality is given and, hence, a misclassification can not be determined (N/A). The second and third bars in each group are representative of medium directionality (3:1 standard deviation ratio) and high directionality (5:1 standard deviation ratio) respectively.

Figure 5.2 and Figure 5.3 depict 100 third moment analyses with parameters set to a sector width of  $10^\circ$  and the maximum radius subdivided into a disc (Figure 5.2) to describe short range directionality and an annulus (Figure 5.3) suggesting long range directionality of equal area. For the patterns generated by an approximately isotropic process, rejection rates varying

Figure 5.2: Single Scale Model, 0 - Radius1, Sector Width=10°.

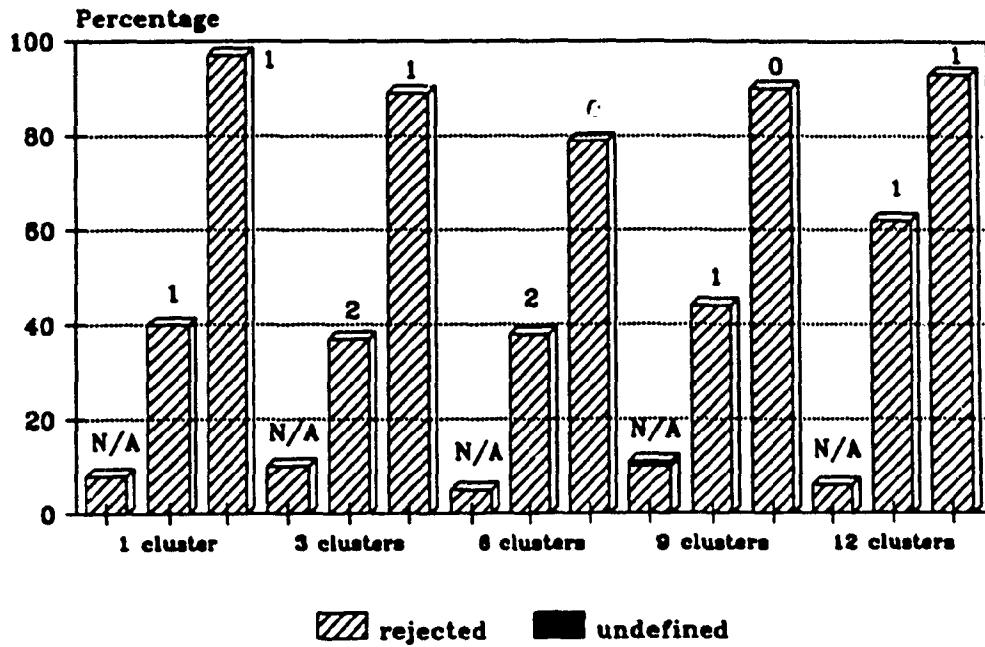
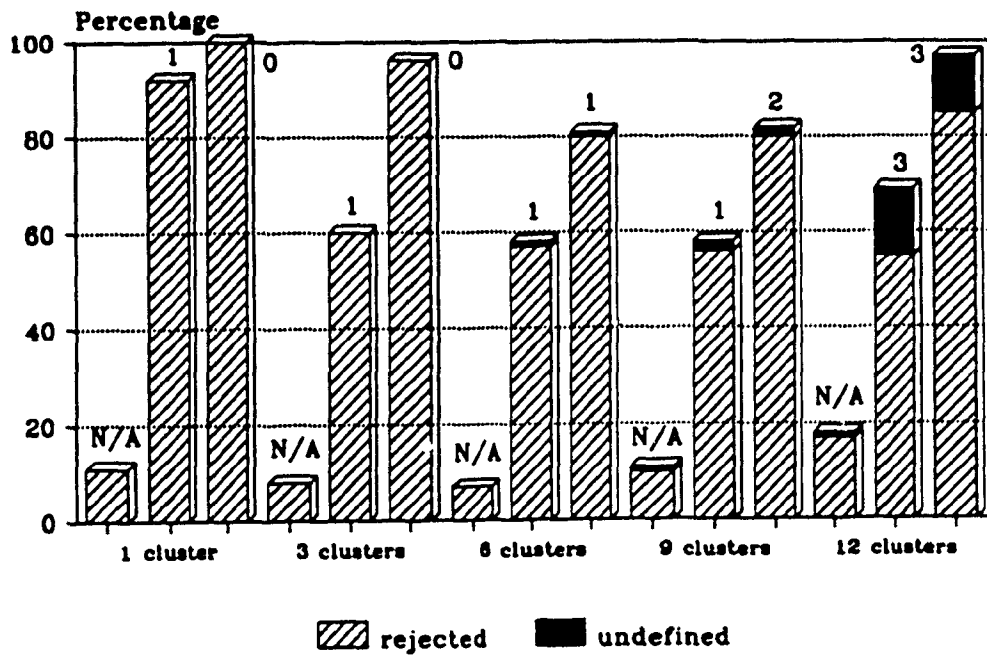


Figure 5.3: Single Scale Model, Radius1 - Radius2, Sector Width=10°.



unsystematically between 5% and 17% are observed in both figures. A clear contrast between short and long range directional distributions can be seen for the medium directional point patterns: The rejection rates increase from 40% to 62% with an increasing number of clusters and decreasing cluster size in Figure 5.2, while the rejection rates drop from 92% to 55% in Figure 5.3. A less clear picture is exhibited for the highly directional point patterns, where the rejection rates in both figures are between 80% and 100%. Undefined percentages are indicative for analyses where the requirements of the chi-square test are not fulfilled. They occur increasingly from the six-cluster case to the twelve-cluster case in the long range directional distributions. This effect is accompanied by increasing average misclassifications of the modal class in the analyses where the null hypothesis of isotropy is rejected.

The influence of a change of parameters on the outcome of third moment analyses is illustrated in Figure 5.4, Figure 5.6, and Figure 5.5. Here, a sectoral angle of  $12^\circ$  was chosen and directional distributions in the short (Figure 5.4), middle (Figure 5.5), and long (Figure 5.6) range are examined. Similar to Figure 5.2 and Figure 5.3, the rejection rates for the isotropic patterns generally vary about 10% for all radii. A strong contrast is apparent for the medium and high directional point patterns between the short range distributions on the one

Figure 5.4: Single Scale Model, 0 - Radius1, Sector Width = 12°.

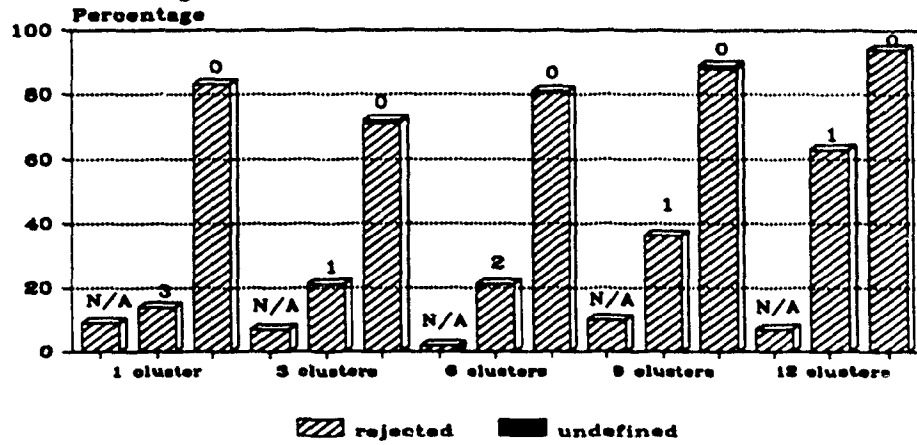


Figure 5.5: Single Scale Model, Radius1 - Radius2, Sector Width = 12°.

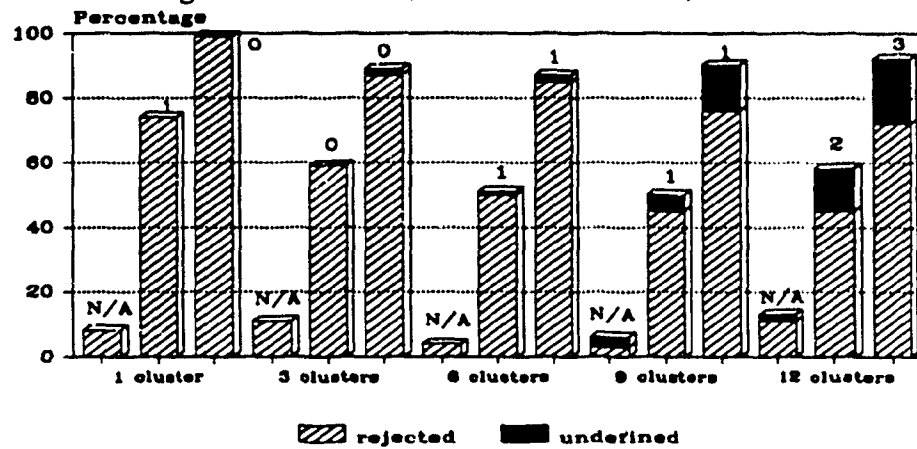
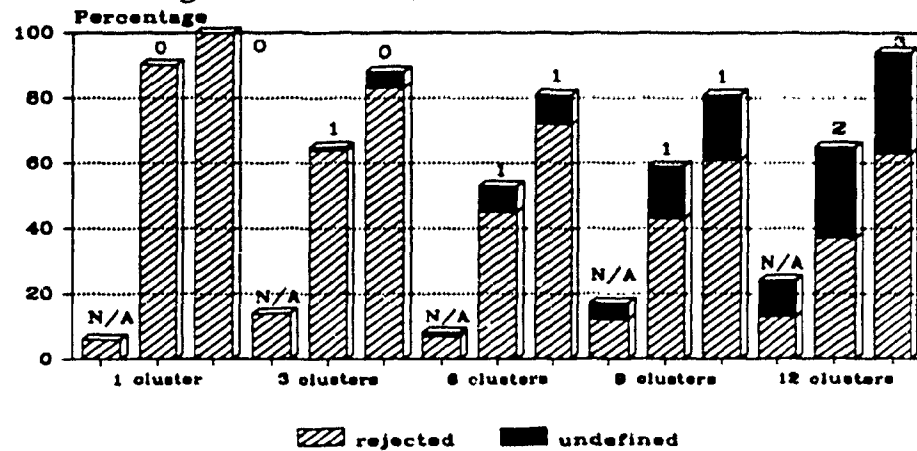


Figure 5.6: Single Scale Model, Radius2 - Radius3, Sector Width = 12°.



hand, and the middle and long range distributions on the other hand. The former exhibit a trend of raised rates of rejection with an increased number of clusters, whereas the latter two show a tendency of declining rejection rates with a decreased cluster size. They also indicate the tighter grouping of points in the smaller clusters. In addition, this tendency is accompanied by an increasing percentage of analyses where the requirements of the chi-square test are not fulfilled, while, when the null hypothesis can be rejected, the modal classes are increasingly misclassified from given orientations. These tendencies are stronger in the long range directional distributions than in the middle range directional distributions. First conclusions can be drawn from the results exhibited in

Figure 5.2 to Figure 5.6. Firstly, as one would expect, it is indicated that in the highly clustered patterns short distance relationships are more representative of directional properties. Secondly, the high misclassifications beyond the short range are indicative of the influence of interactions between the clusters on the location of the modal class in the directional distribution. Thirdly, the impact of void spaces unoccupied by points between the clusters becomes important in the middle and long range directional distributions. They may lead to a violation of the requirements of the chi-square test and, hence, a null hypothesis can neither be accepted nor be rejected.

Although the examination of short, middle and long range directional distributions give some indications about the general behaviour of the third moment method when applied to clustered monodirectional point patterns, it becomes necessary to subdivide the disc of the maximum radius into four equal area zones in order to capture more of the complexity built into the patterns. Figure 5.7 to Figure 5.10 depict the results of applications with radii calculated according to the rules suggested above and a sector width of  $15^\circ$ . In general, the same trends as in Figure 5.2 to Figure 5.6 are displayed, yet individual observations for each case of directional clustering can be made. The bars for the simulations generating only one cluster show an increase of the rejection rate for directional patterns with increasing distance. This effect, which is particularly obvious for the medium directional point patterns, indicates that the consequences of anisotropy in a simple, one-cluster pattern become increasingly important when the angular relations of points more distant to each other are examined. The influence of clustering is already picked up for the three-cluster case as the figures attest. Indicators are raised rejection rates in the short range and smaller rejection rates in the outer ranges in comparison with the one-cluster case. Inspected by itself, the three-cluster analyses still show long and middle range directionalities dominating over short range directionalities. An interesting

**Figure 5.7: Single Scale, 0 - R1, Width=15°. Figure 5.8: Single Scale, R1-R2, Width=15°.**

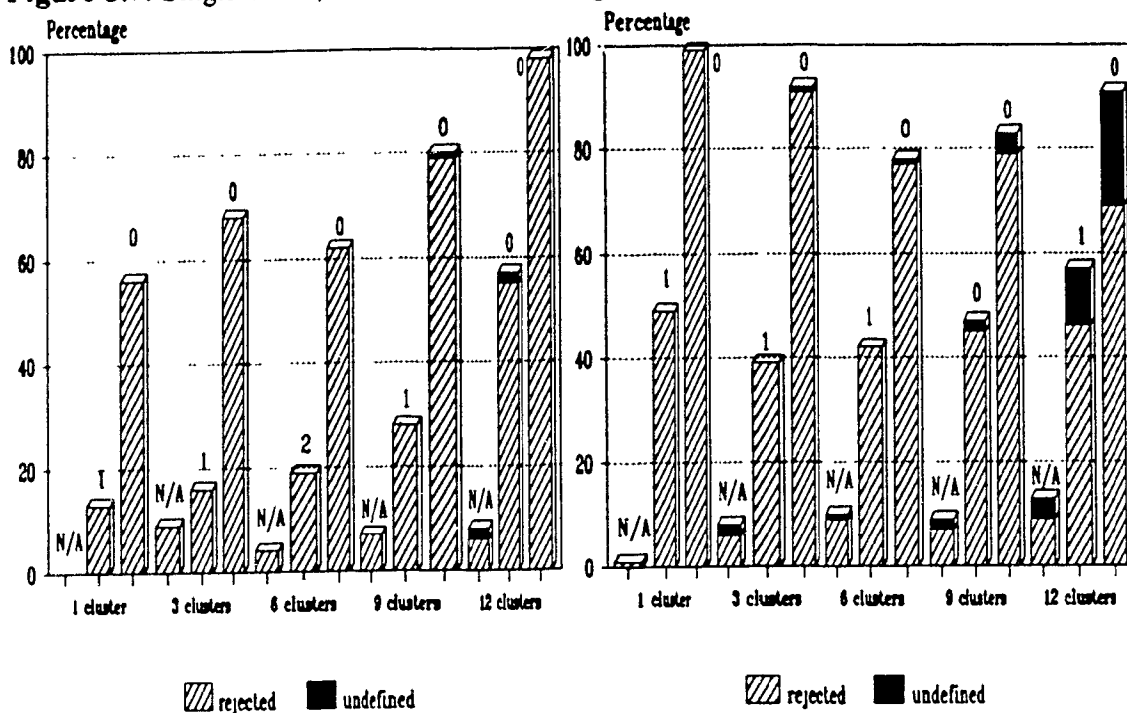
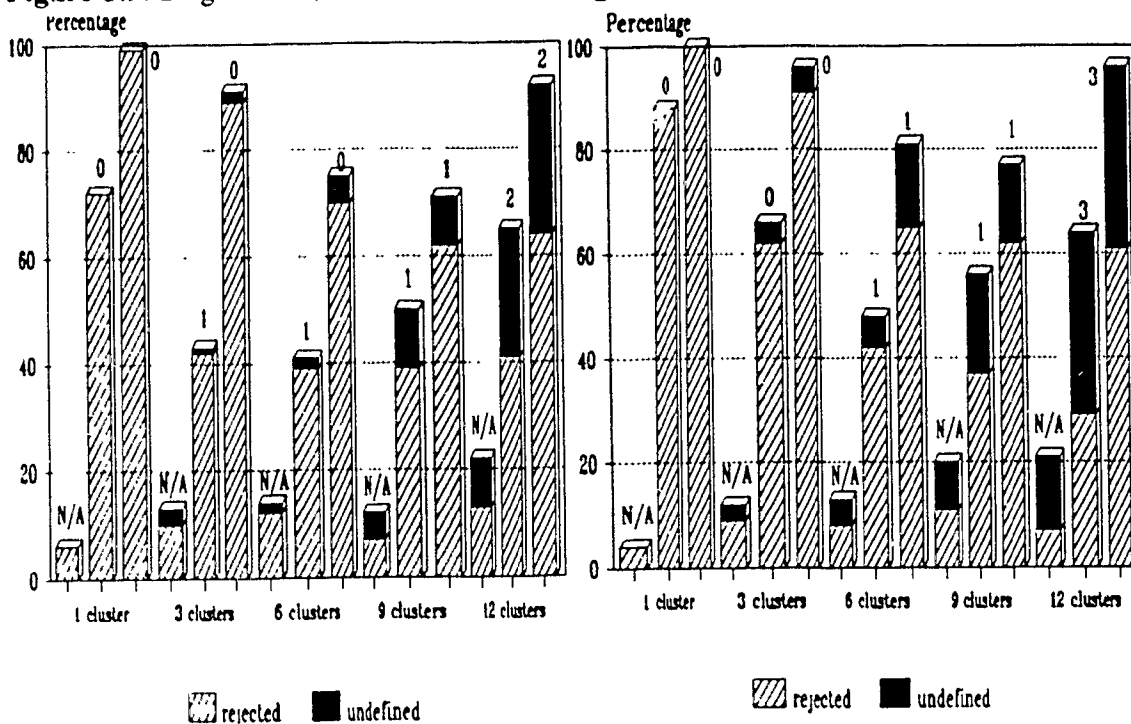


**Figure 5.9: Single Scale, R2-R3, Width=15°. Figure 5.10: Single Scale, R3-R4, Width=15°.**



behaviour is depicted by the six-cluster case. Its rejection rate is increasing from Figure 5.7 to Figure 5.8, and then drops in the outer ranges. Thus, recognizable clustering is shown with still relatively large cluster sizes. However, the rejection rates do not exceed the 80% mark at all, indicating that on the levels of intermediate clustering the interaction between clusters may cover an anisotropic bias contained within the clusters. The same low rejection rates are observed for the nine-cluster case, where percentages for the highly directional patterns are about 80% in both Figure 5.7 and Figure 5.8, then drop in the outer ranges. This behaviour, in addition to the raised detection of void spaces between clusters and higher misclassifications in the outer ranges show the response of the third moment method to increased clustering and smaller cluster sizes. Finally, the results of the twelve-cluster case reveal the ability of the third moment method to detect the given properties built into simulated point patterns. Figure 5.7 with a rejection rate of 99% for the highly directional patterns shows that anisotropy is now important only in the short range. In the ranges beyond the rejection rates drop sharply while undefined percentages and misclassifications become more important. The medium directional distributions parallel this behaviour on a smaller magnitude except in Figure 5.10, where undefined percentages even exceed rejection percentages.

All in all, the third moment method performs acceptably well on the point patterns with an anisotropic bias given on one level of scale. The consistent detection of about 10% of anisotropy in the approximately non-directional point patterns is small enough to be neglected. The results for the highly directional point patterns give strong evidence that while deviations from isotropy are identified, other deviations from homogeneity such as clustering are indicated as well. The strength of this ability is weakened if interaction between the clusters takes place on the same range of distances which define anisotropy within the clusters. It should also be noted that the general trends for the point patterns generated from a higher standard deviation ratio follow those of the appropriate highly directional point patterns on a lower magnitude. Thus, the third moment method is sensitive to variations in the strength of a directional bias.

#### The Identification of a Second Direction

Since the third moment method performed well on point patterns with directionality given on one level, the next step is taken to evaluate the behaviour of point patterns where an anisotropic bias is given on two levels with orthogonal orientations  $\Phi$  and  $\Phi+\pi/2$ . The examination of preliminary analyses carried out on point patterns generated with the standard deviations given in

Table III gave evidence, that the directional distributions  $\theta_{r1,2}(\alpha)$  tend to be bimodal with a major and a secondary modal class. Thus, the procedure designed to find the difference between the mode and the given orientation had to be altered in order to accommodate the secondary mode. Firstly, the two modes have to be identified. For the major modal class, an obvious choice is the class with the largest frequency in the directional distribution. However, with regard to the secondary mode care has to be taken since if the number of classes is sufficiently large, the second highest frequency may well be found close to the major mode, as part of the symmetrical distribution about it. In turn, a secondary mode may have a frequency quite lower than that of the overall second highest frequency, but, since the given orientations are orthogonal one would expect the secondary mode to be quite distant from the primary one. Given the number of classes  $k$ , a reasonable minimum distance from the major modal class appeared to be  $k/5$  classes beyond which a secondary modal class can be identified. Having identified the two modal classes, the misclassifications of the major mode to the regional orientation  $\Phi$  and of the secondary mode to the local orientation  $\Phi+\pi/2$  can be measured. A problem of misidentification may arise if the major mode is representative of the local orientation and the secondary mode shows the regional orientation, which is indicated by large misclassification values. To resolve this problem and identify the maxima

properly the following approach is taken: If both misclassifications exceed a value of  $\text{int}(k/4)+1$  the primary mode is defined as being representative of the local direction while the secondary mode indicates the regional orientation, and their misclassification values are recalculated accordingly.

After altering the classification procedure 100 analyses were carried out for each of the 5 directional scenarios summarized in Figure 4.17. According to the overall intensity of points and the results gained from the analyses on the monodirectional point patterns, the parameters for the third moment method were configured to be four radii delimiting a disc and three annuli of equal area to be intersected by wedges with a sectoral angle of  $6^\circ$ . The results of these analyses are displayed in Figure 5.11 to Figure 5.14. Compared to the figures of the monodirectional analyses they have the additional feature to show, whether the primary or the secondary modal class is representative of the regional direction. Thus, each bar is composed of the percentage where a chi-square test could not be carried out and the percentage of rejections of the null hypothesis of isotropy on the 0.05 significance level, which itself is subdivided into the percentage where the primary mode is indicative of the regional orientation, and the

Figure 5.11: Double Scale, 0-R1, Width=6°. Figure 5.12: Double Scale, R1-R2, Width=6°.

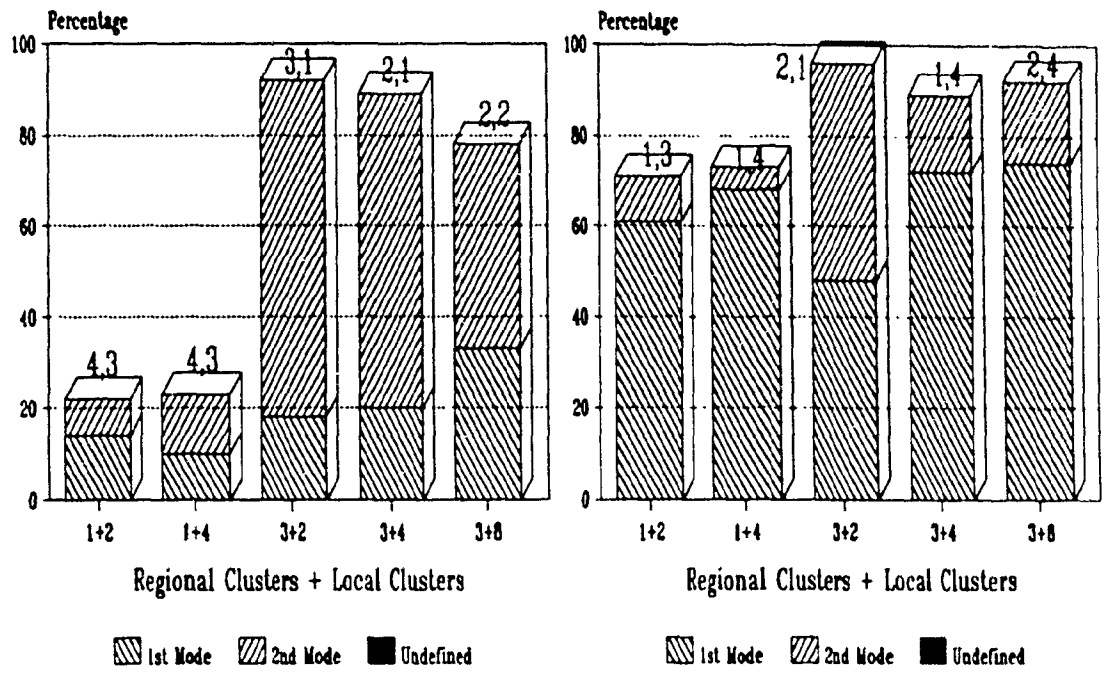
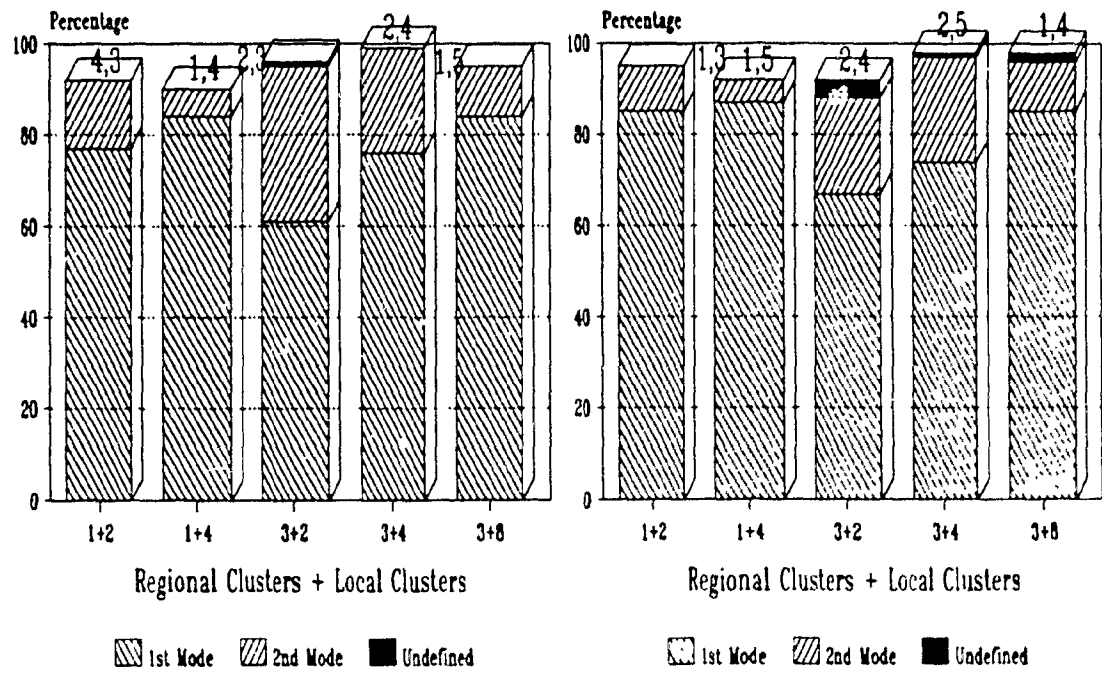


Figure 5.13: Double Scale, R2-R3, Width=6°. Figure 5.14: Double Scale, R3-R4, Width=6°.



percentage where the secondary mode indicates  $\Phi$ . On top of each bar, the average number of classes deviating from the given orientations are given for both modes.

On first glance, the behaviour of the monodirectional single cluster patterns is even more emphasized by the patterns with one regional cluster. The dominance of long distances as carriers of anisotropy on the regional scale is clearly depicted by the increase of the rejection rates from about 22% to 95% from the short range to the outer ranges. It seems that the second direction incorporated into the patterns is not at all picked up since the overall rejection rate for the minimum disc is very low and the average misclassifications for the local directions are quite high. This observation is supported by the fact that the increase from two to four local clusters resulted in a mere overall decrease of 2% of rejections from the former to the latter case in all four figures. A plausible explanation for this behaviour is that both orthogonal directional trends interfered in the short range distributions, an effect that not only made the modal classes indistinguishable but also suggested a uniform directional distribution.

A more characteristic representation of the two levels of directionality by the third moment method is found for the patterns with three regional clusters.

In general, the high overall rejection rates are a first observation. They indicate that anisotropy occurs over the whole range of distance intervals examined. Secondly, for the short range distributions, depicted in Figure 5.11, the major modal class is generally found to be representative of the local orientations more often than being representative of the regional orientation. The lower misclassification values of the local orientation in Figure 5.11 if compared to the values in Figure 5.12 to Figure 5.14 support this observation. Concerning the behaviour of the third moment method with regard to an increase in the number of local clusters, one can generally see the growing importance of regional orientations. At the same time, the local orientations represented by the primary modal class are decreasing. While the properties of the point patterns are reflected in the three annuli by this behaviour, the drop of the overall rejection rates within the short range indicate that the smallest radius in about 15% of the cases with 8 local clusters was not small enough to permit an assignment of the primary modal class to the appropriate orientation.

It can thus be concluded, that in addition to detect varying strengths of an anisotropic bias in general and to indicate clustering, the third moment method also has the ability to distinguish between at least two given orientations. This last quality is particularly dependent upon choosing distance intervals as radii

that somehow reflect the nature of the point pattern. Although the choice of intervals creating a disc and annuli of equal area generally proved to be an appropriate rule of thumb, in some cases slightly better results may be acquired after examining the point pattern to be analyzed by eye and determining the distance intervals empirically.

Finally, some suggestions concerning the interpretation of directional distributions  $\theta_{r1r2}(\alpha)$  of empirical point patterns are given. In general, if the null hypothesis of isotropy is accepted for the short range but rejected for the outer ranges, evidence is given for directionality occurring throughout the entire point pattern being one cluster. A similar conclusion can be drawn, if the null hypothesis is rejected in all intervals, but the chi-square values are increasing in the outer ranges. In this case, the modal classes of the outer ranges will be more reliable indicators of the orientation of an anisotropic bias. If on the other hand the null hypothesis is rejected between the origin and the first radius, while this tendency is lessened in the outer ranges and the chi-square test eventually becomes unfeasible in this domain, one would identify the point pattern as being highly clustered with an anisotropic bias contained within the clusters. In this case, the modal classes of the shorter ranges will display a more precise representation of the orientation. A second modal class is clearly a sign of

secondary directionality. If the roles of the primary and the secondary mode are becoming reversed with increasing radii, the mode being the primary one in the short range distribution and the secondary one in the longer range distributions is representative of directionality on a more local scale. It should also be noted, that the primary mode will have a tendency to display the orientation more precisely than the secondary modes.

## Chapter 6: Conclusions

### Summary

The goal of this study was the evaluation of the blunt-triangle method and the third moment method for their potential of detecting the directional characteristics of spatial point patterns. This goal was accomplished by developing an operational point process model with the capability of incorporating varying degrees of directionality.

The design of this model was based on the observation on empirical geographical point patterns. They indicate that directional properties are often exhibited by the clustering of points around linear features. It seemed thus appropriate to modify an existing stochastic cluster point process toward the generation of elongated, elliptical clusters representative of directional conditions. In order to control the realizations of the model the number, shape, and orientation of clusters were taken as deterministic components in the model. Since geographical point patterns often show varying properties on different levels of spatial resolution, some realizations of the model added directionality on a local scale to the overall regional scale directional properties. The

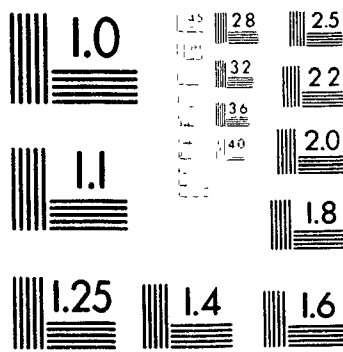
outcomes of applications of the methods to various realizations of the model were then examined with regard to the successful exposition of the built-in properties.

The blunt-triangle method is based on linking all points of a point pattern under study to form a set of triangles. Under the assumption of randomness the mean and the variance of the number of triangles that are blunt within a given tolerance level can be computed. If the number of triangles in the examined pattern which are identified as being blunt exceeds the number of blunt triangles expected with 95% confidence in a random pattern, the point pattern of interest is identified as anisotropic. The results of applications of the blunt-triangle method to the directional cluster point process model showed little or no correspondence to the properties produced in the various realizations of the model. This failure can be explained by the derivation of the blunt-triangle statistics from assumptions of randomness; with the consequence, that applications of this method to non-random patterns result in non-sensical findings. Thus, the blunt-triangle method can not be generally recommended for applications in Geography. If, however, a geographer suspects a point pattern identified as random by quadrat or nearest-neighbour method to have a directional bias, the blunt-triangle method might be used for further exploration

2

OF/DE

2



*MICRO*

of the data set.

The third moment method proceeds by finding directional distributions derived from the number of points counted in certain distance and orientation intervals from each point in the pattern. Non-uniformity of these directional distributions reveals anisotropy, while modal classes in the distributions are indicative of preferred orientations. Throughout the applications of the third moment method to the various realizations of the directional cluster point process model it has been shown that the success of the method is directly dependent upon the proper choice of the distance and orientation intervals that underlie the directional distributions. If appropriate choices for these parameters are made a given directional bias is revealed and its orientation identified with sufficient accuracy. In addition, properties such as clustering and the strength of the directional bias are indicated as well. Although some suggestions pertaining to a rational choice of the parameters for the third moment method are given in this study, it seems that this choice may to some extent be up to the intuition and experience of the researcher with regard to particular point patterns. Nevertheless, it appears that the third moment method has the potential to become a valuable part of the spatial analyst's toolbox, and that more can be learned about the determination of its parameters by applications to real-world

situations.

### **Future Research**

This thesis has provided some insight into the nature of approaches geared toward the identification of directional characteristics of spatial point patterns. By evaluating two recent statistical procedures questions pertaining to the validity of these methods for the solution of certain problems in Geography have been answered. However, some issues relating to these problems were beyond the scope of this study, other questions arose during the research. One limitation of the study is given by the choice of a cluster point process as the starting point of the directional point process model. This choice was justified by the frequent occurrence of clustered point patterns, and by the ease of comprehending an associated directional bias. Nevertheless, the concept of regular point patterns is of some importance in Geography and, thus, an evaluation of the blunt-triangle method and the third moment method based on a directional regular point process might be valuable.

A future possibility for the directional cluster point process can be seen in the transformation from the operational state to a theoretical state by removal

of its deterministic components. By devising a way to estimate its parameters from an empirical point pattern, the directional cluster point process could then serve as part of a method to identify directionality. One may think about the blunt-triangle method which, although intuitively appealing, was determined to fail because of its dependence on assumptions of randomness. Deriving the blunt-triangle statistics from a more appropriate model, perhaps by simulation, would make this method more attractive. However, these tasks may be more appealing to the statistician than to the geographer. Finally, the author could see the future of the third moment method in an increased number of applications. The nature of this method and its dependence upon the external choice of parameters suggest its modification for implementation in the interactive environment of a geographical information system.

Appendix

```

*****
c           Analysis of Directional Point Patterns
c This program proceeds by generating 100 directional point patterns.
c These point patterns are then analysed by the blunt-triangle method and
c the third moment method method with parameters set to 4 radii and a
c sector width of 6 degrees. Results are summarized as percentages of the
c rejection of the null hypothesis of isotropy.
c
c written in UNIX FORTRAN 77 XLA +
c                               by Rolf Puchtinger, 1989.
c
c
*****
c
c           Program directiontest
c           real rad(5),sta1(2),sta2(2)
c           integer idiff(10,100),idif(8),ivalu(3),iperc(5,2),idev(5,2),ivoi(5)
c           integer nops(2),negs(2),lambda(2)
c           character*28 date
c           common /meb1/point(150,2)
c           common /meb2/distan(150,150)
c           common /meb3/freqmat(150,150)
c
c print time and date
c
c           call system('date > dafil')
c           open(1,file='dafil',access='sequential',form='formatted')
c           rewind 1
c           read(1,2)date
c           2 format(a28)
c           print *,date
c
c open file to dump general results
c call system ('rm condout')
c open (9,file='condout')
c
c determine constant PI
c pi=acos(-1.)
c

```

```

c input parameters
  read *,lambda(1),sta1(1),sta2(1)
  read *,lambda(2),sta1(2),sta2(2)
c
c initialize the counting arrays
  do 76,iclo=1,10
    do 78,icli=1,100
      idiff(iclo,icli)=999
78    continue
76    continue
  data nops,negs/0,0,0,0/
c
c *****
c
c loop through the 100 simulations with rotation of the
c point patterns increasing by 20 degrees
c
c *****
c
  isim=0
  do 901,nrot=0,180,20
    do 909,isam=1,10
      isim=isim+1
      write(9,*) 'loop,no',isim
c
c sample the point pattern
  call sampo(lambda,sta1,sta2,numact,nrot,pi)
  write(9,*)'points: ',numact
c
c create the distance-angle matrix
  call corconv (numact,pi)
c
c determine the broadbent-factor
  call broadb(numact,brofa,rad)
  write(9,*) 'brofa:',brofa,' radi',rad
c
c perform the alignment analysis
  call alignm(numact,brofa,pi,maxn,nops,negs)
  write(9,*) 'alignment',maxn,nops,negs
c
c test the orientation of blunt triangles
  call orient(numact,maxn,pi,ivalu,nrot)
  write(9,*) 'orientations',ivalu
  idiff(1,isim)=ivalu(1)

```

```

        idiff(2,isim)=ivalu(2)
c
c perform a third moment analysis
    call thordord(numact,pi,idif,nrot,rad)
    write(9,*) 'thordord: ',idif
    do 8,i=3,10
        idiff(i,isim)=idif(i-2)
    8    continue
c
909    continue
901    continue
c
c*****
c summarize the results
c
        jan=0
    do 47, ian=1,9,2
        jan=jan+1
        ian3=ian+1
        iperc(jan,1)=0
        iperc(jan,2)=0
        idev(jan,1)=0
        idev(jan,2)=0
        ivoi(jan)=0
    do 49,ian2=1,100
        if (idiff(ian,ian2).eq.777) then
            ivoi(jan)=ivoi(jan)+1
            goto 49
        endif
        if (idiff(ian,ian2).ne.999) then
            if (idiff(ian,ian2).ge.8.and.idiff(ian3,ian2).ge.8) then
                idev(jan,2)=idev(jan,2)+(15-idiff(ian,ian2))
                idev(jan,1)=idev(jan,1)+(15-idiff(ian3,ian2))
                iperc(jan,2)=iperc(jan,2)+1
            else
                iperc(jan,1)=iperc(jan,1)+1
                idev(jan,1)=idev(jan,1)+idiff(ian,ian2)
                idev(jan,2)=idev(jan,2)+idiff(ian3,ian2)
            endif
        endif
    49    continue
        ntoper=iperc(jan,1)+iperc(jan,2)
        idev(jan,1)=ndevi(idev(jan,1),ntoper)
        idev(jan,2)=ndevi(idev(jan,2),ntoper)

```

```

47  continue
c
c*****
c output the results
c
  print 172,'regional clusters= ',lambda(1),' std1= ',
& sta1(1),' std2= ',sta2(1)
  print 172,'local clusters= ',lambda(2),' std1= ',
& sta1(2),' std2= ',sta2(2)
172  format(1x,a25,i3,a12,f4.0,a12,f4.0)
    print *
    print *
    print *,'KENDALLS METHOD OF BLUNT TRIANGLES'
    print *
    print *,'                elliptical    rectangular'
    print *,'triangles exceeding 2 standard deviations:',nops(1),nops(2)
    print *,'triangles less than 2 standard deviations:',negs(1),negs(2)
    print *
    print *
    print *,'ORIENTATION OF TRIANGLES > 170 DEGREES'
    print *
    print 155,iperc(1,1),idev(1,1),iperc(1,2),idev(1,2)
    print *
    print *
    print *,'THIRD MOMENT ANALYSIS'
    print *
    print *,'radii                deviations'
    numpsi=0
    do 189,nco=2,5
    print *
    numpsi=numpsi+1
    print *,'Annulus no. ',numpsi
    print 155,iperc(nco,1),idev(nco,1),iperc(nco,2),idev(nco,2),ivoi(nco)
    print *
189  continue
    print 9
9    format('1')
155  format(1x,'Scale1: ',i3,' Misclass: ',i2,
&      8x,'Scale2: ',i3,' Misclass: ',i2,
&      8x,'undefined: ',i2)
179  format(1x,a7,3(30i4/7x),10i4)
    close(9)
    stop
    end

```

```

c
c *****
c subroutine to transform x/y-coordinates into a matrix
c with distances in the upper triangle and angles in
c the lower triangle
c *****
      subroutine corconv(na,pi)
      common /meb1/p(150,2)
      common /meb2/angmat(150,150)
c
c reset the distance/angle matrix
c
      do 32,iset=1,150
      do 42,nset=1,150
          angmat(nset,iset)=0
42      continue
32      continue
      do 45,j=1,(na-1)
          angmat(j,j)=0.0
      do 56,k=(j+1),na
c
          xval=p(j,1)-p(k,1)
          yval=p(j,2)-p(k,2)
          if (yval.eq.0) then
              angmat(k,j)=pi
              goto 68
          endif
          angvalu=atan(xval/yval)
          angmat(k,j)=pi/2-angvalu
68      angmat(j,k)=sqrt(xval**2+yval**2)
56      continue
45      continue
      return
      end
c
c *****
c subroutine to determine the broadbent-factor
c and the radii for the third moment method
c *****
      subroutine broadb(na,b,radu)
      real radu(5)
      common /meb1/p(150,2)

```

```

c generate the variance-covariance matrix
  var1=0
  cor1=0
  var2=0
  cor2=0
  covar=0
  do 10,j=1,na
    var1=var1+p(j,1)**2
    cor1=cor1+p(j,1)
    var2=var2+p(j,2)**2
    cor2=cor2+p(j,2)
    covar=covar+p(j,1)*p(j,2)
10  continue
  var1=(var1-cor1**2/na)/(na-1)
  var2=(var2-cor2**2/na)/(na-1)
  covar=(covar-(cor1*cor2)/na)/(na-1)
c
c determine the broadband factor from the eigenvalues of
c the variance-covariance matrix
c
  rtex=sqrt((var1-var2)*(var1-var2)+4.*covar*covar)
  aval=var1+var2
  b=0.5*(sqrt((aval+rtex)/(aval-rtex))+sqrt((aval-rtex)/(aval+rtex)))
c
c compute radii for the third moment analysis
c
  radu(1)=0.
  do 177,ilx=2,5
    radu(ilx)=sqrt((ilx-1)*aval*0.25)
177 continue
c
c
  return
  end
c *****
c function to compute factorials
c
  double precision function fact(n,m)
  fact=1.
  do 12,i=n,m
    fact=fact*i
12  continue
  return
  end

```

```

c *****
c subroutine to perform an alignment analysis using distances
c from the distance\angle-matrix
c *****
c
c      subroutine alignm(na,br,pi,maxnum,npos,nneg)
c      common /meb2/distang(150,150)
c      common /meb3/freqdir(150,150)
c      integer icol,irow1,irow2,npos(2),nneg(2)
c      double precision fact
c
c      compute combinatorials
c      comb(n,m)=fact((n-m+1),n)/fact(1,m)
c
c      maxnum=0
c      do 46,kval=1,150
c      do 118, klop=1,150
c          freqdir(klop,kval)=0
118  continue
46   continue
c      degtorad=pi/180.
c
c      initialize the computation of the standard deviations
c
c      trinu=comb(na,3)
c      epsilon=10.*degtorad
c
c      elliptical convex hull
c
c      zlambda = br/pi
c      zlambda = zlambda*zlambda
c      expr3=comb(na-3,2)*3.*((br**2*0.1103275111-0.0075052729)-zlambda)
c      expr4=comb(na-3,1)*3.*(br**2*0.1801265487-0.0600421829)-zlambda
c      expec=epsilon*trinu*zlambda
c      ergebn=2*sqrt(abs(expec +epsilon**2*(-zlambda+expr3+expr4)*trinu))
c      posel=expec+ergebn
c      meel=expec-ergebn
c
c      rectangular convex hull
c
c      zlambda = br/3.
c      zlambda = zlambda*zlambda
c      expr3=comb(na-3,2)*3.*((br**2*0.1160346836-0.0032940654)-zlambda)
c      expr4=comb(na-3,1)*3.*((br**2*0.1896296296-0.0553086420)-zlambda)

```

```

    expec=epsilon*trinu*zlambda
    ergeb=2*sqrt(abs(expec +epsilon**2*(-zlambsq+expr3+expr4)*trinu))
    posre=expec+ergeb
    mere=expec-ergeb
c
c loop through all distances
c
    do 10,icol=1,na-2
    do 20,irow1=icol+1,na-1
    do 30,irow2=irow1+1,na
c find the longest distance
        if (distang(icol,irow1).gt.distang(icol,irow2).and.
&          distang(icol,irow1).gt.distang(irow1,irow2)) then
            bigdist=distang(icol,irow1)
            sdist=distang(icol,irow2)
            tdist=distang(irow1,irow2)
            mecol=icol
            merow=irow1
        elseif (distang(icol,irow2).gt.distang(irow1,irow2).and.
&          .distang(icol,irow2).gt.distang(icol,irow1)) then
            bigdist=distang(icol,irow2)
            sdist=distang(irow1,irow2)
            tdist=distang(icol,irow1)
            mecol=icol
            merow=irow2
        else
            bigdist=distang(irow1,irow2)
            sdist=distang(icol,irow1)
            tdist=distang(icol,irow2)
            mecol=irow1
            merow=irow2
        endif
c
c determine the blunt angle under consideration of rounding errors
c
    if (sdist+tdist.le.bigdist) then
        bigangle=pi
        goto 44
    endif
    brex=(sdist**2+tdist**2-bigdist**2)/(2*sdist*tdist)
    if (brex.gt.1.or.brex.lt.-1) then
        bigangle=pi
        goto 44
    endif

```

```

        bigangle=acos(brex)
c
c determine the number of triangles between 170 and 180 degrees
c
44  sysangle = pi - epsilon
    if (bigangle.ge.sysangle) then
        maxnum = maxnum +1
        freqdir(mecol,merow)=freqdir(mecol,merow)+1
    endif
c
30  continue
20  continue
10  continue
c
    if (maxnum.gt.posel) npos(1)=npos(1)+1
    if (maxnum.lt.rneel) nneg(1)=nneg(1)+1
    if (maxnum.gt.posre) npos(2)=npos(2)+1
    if (maxnum.lt.rnere) nneg(2)=nneg(2)+1
c
    return
    end
c
c *****
c subroutine to test for orientation of the blunt angles
c *****
c
    subroutine orient(nb,maxnum,pi,ipass,nrot)
    integer ipass(3),icount(30)
    common /meb2/ angmat(150,150)
    common /meb3/freqdir(150,150)
    nu=30
    radtodeg = 180./pi
c
c classify angle
c
    klasi=klas(nu,nrot)
    if (nrot.le.90) then
        mozz=klas(nu,nrot+90)
    else
        mozz=klas(nu,nrot-90)
    end if
c
c initialize the frequency vector
c

```

```

        do 123,ini=1,nu
            icount(ini)=0
123    continue
c
        sinsum=0.
        cosum=0.
        nasu:=0
157    do 76, jlo1=1,(nb-1)
        do 78, jlo2=(jlo1+1),nb
c
            if (freqdir(jlo1,jlo2).eq.0.) goto 78
            sinc= sin(angmat(jlo2,jlo1)*2.)
            cosc=cos(angmat(jlo2,jlo1)*2.)
c
            sinsum=sinsum+sinc
            cosum=cosum+cosc
            nasu=nasu+1
c
c classify the number of angles
c
            index = 0
            do 135, inlp=6,180,6
                index = index+1
                angle=angmat(jlo2,jlo1)*radtodeg
                if (angle.le.inlp.and.angle.gt.(inlp-6))
                    & icount(index) = icount(index) + 1
135    continue
78    continue
76    continue
c
c compute chi-square statistic
        bignum=0.
c
        expe=real(nasu)/real(nu)
        incr=0
        chisq=0.
        do 891,is=1,nu
            chisq=chisq+(((icount(is)-expe)**2)/expe)
891    continue
c
c find the modal classes and their deviations
c
        if (chisq.le.42.557) then
            ipass(1)=999

```

```

        ipass(2)=999
        goto 895
    endif
    call findmod(nu,icount,mod1,mod2)
    ipass(1)=idiffer(nu,klasi,mod1)
    ipass(2)=idiffer(nu,mozz,mod2)
    write(9,*)'modes' ,mod1,mod2,'diffs' ,ipass,'angles: ',klasi,mozz
    write(9,*)icount
    write(9,*)
c
c compute summary statistics
c based on the mean vector and the Rayleigh-test (zstat)
c
895  amean=atan(sinsum/cosum)
    if (cosum.lt.0.) then
        amean=(pi+amean)*0.5
    else if (cosum.gt.0.and.sinsum.gt.0.) then
        amean=amean*0.5
    else
        amean=amean*0.5+pi
    endif
    amean=amean*radtodeg
    vectlen=sqrt(sinsum*sinsum+cosum*cosum)/nasu
    zstat=vectlen*vectlen*nasu
    ipass(3)=abs(nrot-int(amean))
    if (ipass(3).gt.90) ipass(3)=180-ipass(3)
    if (zstat.le.6.91) ipass(3)=999
c
c
    return
    end
c
c *****
c third moment analysis
c (4 directional distributions, sector width = 6 degrees)
c *****
c
    subroutine thirdord(na,pi,ndif,nrot,radi)
    real pinum(4),chis(4),expe(4),radi(5)
    integer ndif(8),frq(4,36),nren(36)
    common /meb2/dira(150,150)
    parameter (nbar=30)
    degtorad=pi/180.
c

```

```

c initialize frequency vectors
c
  do 252, init=1,4
    do 600,init2=1,nbar
      frq(init,init2)=0
600  continue
252  continue
c
c classify rotation angle
c
  klasi=klas(nbar,nrot)
  if (nrot.le.90) then
    mozz=klas(nbar,nrot+90)
  else
    mozz=klas(nbar,nrot-90)
  end if
  step=pi/real(nbar)
c
c derive directional distributions
c
  do 255, lp1=1,(na-1)
    do 257, lp2=(lp1+1),na
      do 253, incra=2,5
c
        do 603,nang=1,nbar
          ang=nang*step
          if (dira(lp1,lp2).gt.radi(incra-1).and.dira(lp1,lp2).le.
& radi(incra).and.dira(lp2,lp1).le.ang
& .and.dira(lp2,lp1).gt.(ang-step))
& frq(incra-1,nang)=frq(incra-1,nang)+1
603  continue
253  continue
257  continue
255  continue
c
c determine the maximum number and chi-square
c
  do 378,loopx=2,8,2
    loop1=int(loopx*0.5)
    pinum(loop1)=0.
    do 604,loop2=1,nbar
      pinum(loop1)=frq(loop1,loop2)+pinum(loop1)
604  continue
    if (pinum(loop1).lt.nbar*5) then

```

```

        ndif(loopx)=777
        ndif(loopx-1)=777
        expe(loop1)=0
        goto 378
    endif
    expe(loop1)=pinum(loop1)/real(nbar)
378  continue
c
c calculate the distribution functions
c
    do 605,ilopx=2,8,2
    ilop1=int(ilopx)*0.5
    if (expe(ilop1).eq.0.) goto 605
    chis(ilop1)=0.
    bigval=0.
c
c inner loop
c
        do 607,ilop4=1,nbar
        chis(ilop1)=chis(ilop1)+(frq(ilop1,ilop4)-
&                expe(ilop1))**2/expe(ilop1)
c
        nren(ilop4)=frq(ilop1,ilop4)
607  continue
c
c find the mode and the second peak
c
    if (chis(ilop1).le.42.557) then
        ndif(ilopx)=999
        ndif(ilopx-1)=999
        goto 605
    endif
    call findmod(nbar,nren,mod1,mod2)
    write(9,*)'modes ',mod1,mod2,klasi
    write(9,*)nren
    ndif(ilopx-1)=idiffer(nbar,klasi,mod1)
    ndif(ilopx)=idiffer(nbar,mozz,mod2)
    write(9,*)ndif,' no: ',ilopx-1,ilopx
605  continue
c
    return
    end
c

```

```

c *****
c subroutine to determine the two modal classes
c *****
c
c      subroutine findmod(n,ndis,mo1,mo2)
c      integer ndis(36),mofi(2),mose(2),most(2)
c
c determine the buffer-size around a mode
c
c      id=nint(n/5.)
c      iu=n-id
c
c initialize intermediate variables
c
c      mofi(1)=0
c      mose(1)=0
c      most(1)=0
c      mofi(2)=0
c      mose(2)=0
c      most(2)=0
c
c
c      do 831,lo=1,n
c          nva=ndis(lo)
c          if (nva.lt.mose(1)) goto 831
c
c          if (nva.eq.mofi(1)) then
c              if (lo-mofi(2).gt.id.and.lo-mofi(2).lt.iu) then
c                  mose(1)=nva
c                  mose(2)=lo
c              else
c                  if (n-lo.gt.mofi(2)) then
c                      mofi(2)=lo+nint((n-lo+mofi(2))*0.5)
c                  else
c                      mofi(2)=mofi(2)-nint((n-lo+mofi(2))*0.5)
c                  end if
c              end if
c          else if (nva.gt.mofi(1)) then
c              most(1)=mofi(1)
c              most(2)=mofi(2)
c              mofi(1)=nva
c              mofi(2)=lo
c              if (mofi(2)-most(2).gt.id.and.mofi(2)-most(2).lt.iu) then
c                  mose(1)=most(1)

```

```

        mose(2)=most(2)
    end if
    else if (nva.eq.mose(1).and.(lo-mofi(2).gt.id.
& and.lo-mofi(2).lt.iu)) then
        if (lo-mose(2).lt.lo-mofi(2)) then
            mose(2)=mose(2)+nint((lo-mose(2))*0.5)
        else
            if (n-lo.gt.mose(2)) then
                mose(2)=lo+nint((n-lo+mose(2))*0.5)
            else
                mose(2)=mose(2)-nint((n-lo+mose(2))*0.5)
            end if
        end if
    else if (nva.gt.mose(1).and.(lo-mofi(2).gt.id.
& and.lo-mofi(2).lt.iu)) then
        mose(1)=nva
        mose(2)=lo
    end if
c
831 continue
c
    if (mofi(2)-iu.ge.mose(2)) then
        mose(1)=0
        mose(2)=0
        do 844,lott=mofi(2)-(iu-1),mofi(2)-(id+1)
            if (ndis(lott).gt.mose(1)) then
                mose(1)=ndis(lott)
                mose(2)=lott
            end if
844 continue
        end if
        mo1=mofi(2)
        mo2=mose(2)
        if (mo1.eq.0) mo1=1
        if (mo2.eq.0) mo2=2
c
    return
    end
c
c *****
c function to determine the difference between a given class and
c another class in a frequency distribution
c

```

```

function idiffer(numb,nang,mode)
idiffer=iabs(mode-nang)
if (idiffer.gt.(numb*0.5)) idiffer=numb-idiffer
write(9,*)'diffi ',idiffer
return
end

c
c*****
c classification of the rotation angle
c
function klas(nbar,nrot)
if (nrot.eq.0) then
    klas=1
    return
endif
clawi=180./real(nbar)
if (mod(nrot,nbar).eq.0) then
    klas=int(nrot/clawi)
else
    klas=aint(nrot/clawi+1)
endif
return
end

c
c*****
c
function ndevi(l,m)
if (m.eq.0) then
    ndevi=888
else
    ndevi=int(l/m)
endif
return
end

c
c*****
c Directional clustered point pattern
c generated from a poisson-bivariate normal process
c with two scales
c*****
c
subroutine sampo(lambda,std1,std2,iobs,irot,pix)
common /meb1/p(150,2)
integer lambda(2)

```

```

real cov(2,2),rsig(2,2),rval(300,2),std1(2),std2(2)
external rnsset,mopt,munf,mpoi,chfac,rnmvn,amach
tol=100.*amach(4)
call rnsset(0)
call mopt(2)
c reset the coordinate array (p)
do 21,i=1,150
    p(i,1)=0
    p(i,2)=0
21  continue
iobs=0

c
c set parameters for regional pattern
c
    roto=irotpix/180.
    theta=60./real(lambda(1))
    lambx=lambda(1)
    isc=1
    nscal=1
    sta1=std1(1)
    sta2=std2(1)
c *****
c main section of point generation
c
c generate the variance-covariance matrix
c
15  cov(1,2)=0.
    cov(1,1)=sta1**2
    cov(2,2)=sta2**2
    cov(2,1)=cov(1,2)

c
    roco=cos(roto)
    rosi=sin(roto)

c
c loop through the number of directional clusters
c
    do 65,iclu=1,lambx
81  call mpoi(1,theta,ir)
    if (ir.eq.0) goto 81

c
c determine the center of the cluster
c
    if (isc.eq.1) then
        xcen=aint(249*rnunf()-125)

```

```

        ycen=aint(249*rnunf()-125)
    else if (isc.eq.2) then
        insec=aint(nscal*rnunf())
        xcen=p(insec,1)
        ycen=p(insec,2)
    endif
c
    call chfac(2,cov,2,tol,irank,rsig,2)
    call rnmvn(300,2,rsig,2,rval,300)
c
c rotate and translate the points
c
    ncount=0
    do 19,loop=1,300
        xrot=(rval(loop,1)*roco-rval(loop,2)*rosi)+xcen
        yrot=(rval(loop,1)*rosi+rval(loop,2)*roco)+ycen
c
c check if point already exists
c
        if (xrot.ge.210.or.xrot.le.-210.or.yrot.ge.210.or.yrot.le.-210)
            & goto 19
        do 111, icheck=1,iobs
            if(p(icheck,1).eq.xrot.and.p(icheck,2).eq.yrot)goto 19
111    continue
c
c check if number of points is reached
c
        ncount=ncount+1
        iobs=iobs+1
c
c sample the point
c
        p(iobs,1)=xrot
        p(iobs,2)=yrot
        if (ncount.eq.ir) goto 65
c
19    continue
65    continue
c
c set parameters for second scale
c
        if (lambda(2).eq.0) isc=2
        if (isc.eq.1) then
            roto=roto+pix*0.5

```

```
        nscal=iobs
        theta=40./real(lambda(2))
        lambx=lambda(2)
        sta1=std1(2)
        sta2=std2(2)
        isc=2
        goto 15
    endif
c
c translate the origin to the lower left corner
c and rescale area to unit size
c
    do 199,lo=1,iobs
        p(lo,1)=(p(lo,1)+210)/420.
        p(lo,2)=(p(lo,2)+210)/420.
199    continue
    return
end
```

### References

- Andrews, J.T., 1965. The Corries of the Northern Nain-Oak Section of Labrador. Geographical Bulletin 7, 129-136.
- Andrews, J.T. and R.E. Dugdale, 1971. Quaternary History of Northern Cumberland Pensinsula, Baffin Island, N.W.T.: Part V: Factors Affecting Corrie Glacierization in Okoa Bay. Quaternary Research 1, 532-551.
- Andrews, J.T., R.G. Barry, L. Drapier, 1970. An Inventory of the Present and Past Glacierization of Home Bay and Okoa Bay, East Baffin Island, N.W.T., Canada, and some Climatic and Palaeoclimatic Considerations. Journal of Glaciology 9, 337-362.
- Batschelet, E., 1981. Circular Statistics in Biology. Academic Press, New York.
- Boots, B.N and R.K. Burns, 1984. Analyzing the Spatial Distribution of Drumlins: A Two-Phase Mosaic Approach. Journal of Glaciology 30, 302-307.
- Boots, B.N. and A. Getis, 1988. Point Pattern Analysis. Sage, Newbury Park.
- Broadbent, S.R., 1980. Simulating the Ley Hunter. Journal of the Royal Statistical Society A143, 109-140.
- Cliff, A.D. and J.K. Ord, 1981. Spatial Processes: Models and Applications. Pion, London.
- Dacey, M.F., 1968. An Empirical Study of the Areal Distribution of Rural Settlements in Puerto Rico using Quadrat Methods. Institute of British Geographers, Transactions, 45, 51-69.
- Day, M., 1971. The Morphology and Hydrology of some Jamaican Karst Depressions. Earth Surface Processes 1, 111-129.
- Diggle, P.J., 1983. Statistical Analysis of Spatial Point Patterns. Academic Press, New York.

- Evans, I.S., 1977. World-Wide Variations in the Direction and Concentration of Cirque and Glacier Aspects. Geografiska Annaler 59A, 151-175.
- Drake, J.J. and D.C. Ford, 1972. The Analysis of Growth Patterns of Two-Generation Populations: The Example of Karst Sinkholes. Canadian Geographer 16, 381-384.
- Gaile, G.L. and J.E. Burt, 1980. Directional Statistics. Geo Abstracts, Norwich.
- Getis, A. and B. Boots, 1978. Models of Spatial Processes. Cambridge University Press.
- Gordon, J.E., 1977. Morphometry of Cirques in the Kintail-Affric-Cannich Area of Northwest Scotland. Geografiska Annaler 59A, 177-194.
- Gould, P.R., 1967. On the Geographical Interpretation of Eigenvalues. Institute of British Geographers, Transactions 42, 53-86.
- Gravenor, C.P., 1974. The Yarmouth Drumlin Field, Nova Scotia, Canada. Journal of Glaciology 13, 45-54.
- Hägerstrand, T., 1965. A Monte Carlo Approach to Diffusion. European Journal of Sociology 6, 43-67.
- Hanisch, K.H., 1983. Reduction of n-th Moment Measures and the Special Case of the third Moment Measure of Stationary and Isotropic Planar Point Processes. Mathematische Operationsforschung und Statistik, Series Statistics 14, 421-435.
- Harvey, D.W., 1968. Pattern, Process, and the Scale Problem in Geographical Research. Institute of British Geographers, Transactions 43, 71-78.
- Haynes, K.E. and W.T. Enders, 1975. Distance, Direction, and Entropy in the Evolution of a Settlement Pattern. Economic Geography 51, 357-365.
- Hill, A.R., 1973. The Distribution of Drumlins in County Down, Ireland. Annals of the Association of American Geographers 63, 226-240.
- Hudson, J.C., 1969. Pattern Recognition in Empirical Map Analysis. Journal of Regional Science 9, 189-200.

- Hudson, J.C. and P.M. Fowler, 1966. The Concept of Pattern in Geography. Department of Geography, University of Iowa, Discussion Paper 1.
- Jauhiainen, E., 1975, Morphometric Analysis of Drumlin Fields in Northern Central Europe. Boreas 4, 219-230.
- Johnson, N.L. and S. Kotz, 1972. Distributions in Statistics: Continuous Multivariate Distributions. John Wiley, New York.
- Kemmerly, P.G., 1982. Spatial Analysis of a Karst Depression Population: Clues to Genesis. Geological Society of America, Bulletin 93, 1063-1188.
- Kendall, D.G. and W.S. Kendall, 1980. Alignments in Two-Dimensional Random Sets of Points. Advances in Applied Probability 12, 380-424.
- Kendall, D.G., 1984. Shape Manifolds, Procrustean Metrics, and Complex Projective Spaces. Bulletin of the London Mathematical Society 16, 81-121.
- Kendall, D.G., 1989. A Survey of the Statistical Theory of Shape. Statistical Science 4, 87-120.
- King, C.A.M., 1974. Morphometry in Glacial Geomorphology. In Coates, D.R. (ed.): Glacial Geomorphology, State University of New York Press.
- King, L.J., 1962. A Quantitative Expression of the Pattern of Urban Settlements in Selected Areas of the United States. Tijdschrift Voor Economische en Sociale Geografie 53, 1-7.
- LaValle, P., 1967. Some Aspects of Linear Karst Depression Development in South Central Kentucky. Annals of the Association of American Geographers 57, 49-71.
- Mardia, K.V., 1972. Statistics of Directional Data. Academic Press, London.
- Matschinski, M., 1968. Alignment of Dolines North-West of Lake Constance, Germany. Geological Magazine 105, 56-61.

- McConnell, H. and J.M. Horn, 1972. Probabilities of Surface Karst. In Chorley, R.J. (ed): Spatial Analysis in Geomorphology. Harper & Row, New York.
- Norcliffe, G.B., 1969. On the Use and Limitations of Trend Surface Models. Canadian Geographer 8, 338-348.
- Ohser, J., 1983. On Estimators for the Reduced Second Moment Measure of Point Processes. Mathematische Operationsforschung und Statistik, Series Statistics 14, 63-71.
- Ohser, J. and D. Stoyan, 1981. On the Second-Order and Orientation Analysis of Planar Stationary Point Processes. Biometrical Journal 23, 523-533.
- Rayner, J.N. and R.G. Golledge, 1972. Spectral Analysis of Settlement Patterns in Diverse Physical and Economic Environments. Environment and Planning 4, 347-371.
- Ripley, B.D., 1976. The Second-Order Analysis of Stationary Point Processes. Journal of Applied Probability 13, 255-266.
- Ripley, B.D., 1977. Modelling Spatial Patterns. Journal of the Royal Statistical Society B39, 172-212.
- Ripley, B.D., 1979. The Analysis of Geographical Maps. In Bartels, C.P.A. and R.H. Ketellaper (eds): Exploratory and Explanatory Statistical Analysis of Spatial Data. Nijhoff, Boston.
- Ripley, B.D., 1979. Tests of "Randomness" for Spatial Point Patterns. Journal of the Royal Statistical Society B41, 368-374.
- Ripley, B.D., 1981. Spatial Statistics. John Wiley, New York.
- Ripley, B.D., 1983. Edge Corrections for Spatial Processes. In Ambartzumian, R.V. and W. Weil (eds): Stochastic Geometry, Geometric Statistics, Sterology. Teubner Verlag, Leipzig.
- Ripley, B.D., 1988. Statistical Inference for Spatial Processes. Cambridge University Press.

- Robinson, G., 1972. Trials on Trends through Clusters of Cirques. Area **4**, 104-113.
- Robinson, G. and K.J. Fairbairn, 1969. An Application of Trend Surface Mapping to the Distribution of Residuals from a Regression. Annals of the Association of American Geographers **59**, 158-170.
- Robinson, G., J.A. Peterson, P.M. Anderson, 1971. Trend Surface Analysis of Corrie Altitudes in Scotland. Scottish Geographical Magazine **87**, 142-146.
- Rose, J. and J.M. Letzer, 1975. Drumlin Measurements: A Test of the Reliability of Data Derived from 1:25000 Scale Topographic Maps. Geological Magazine **112**, 361-371.
- Small, C.G., 1982. Random Uniform Triangles and the Alignment Problem. Mathematical Proceedings of the Cambridge Philosophical Society **91**, 315-322.
- Small, C.G., 1988. Techniques of Shape Analysis on Sets of Points. International Statistical Review **56**, 243-257.
- Smalley, I.J. and D.J. Unwin, 1968. The Formation and Shape of Drumlins and their Distribution and Orientation in Drumlin Fields. Journal of Glaciology **7**, 377-390.
- Stoyan, D., W.S. Kendall, J. Mecke, 1987. Stochastic Geometry and its Applications. John Wiley, New York.
- Sugden, D.E., 1969. The Age and Form of Corries in the Cairngorms. Scottish Geographical Magazine **85**, 34-46.
- Trenhaile, A.S., 1971. Drumlins: Their Distribution, Orientation, and Morphology. Canadian Geographer **15**, 113-126.
- Trenhaile, A.S., 1975. The Morphology of Drumlin Fields. Annals of the Association of American Geographers **65**, 297-312.
- Trenhaile, A.S., 1975. Cirque Elevation in the Canadian Cordillera. Annals of the Association of American Geographers **65**, 517-529.

- Trenhaile, A.S., 1976. Cirque Morphometry in the Canadian Cordillera. Annals of the Association of American Geographers 66, 451-462.
- Unwin, D.J., 1973. The Distribution and Orientation of Corries in Northern Snowdonia, Wales. Institute of British Geographers, Transactions 58, 85-97.
- Upton, G. and B. Fingleton, 1985. Spatial Data Analysis by Example Vol.1. John Wiley, New York.
- Upton, G.J.G., 1986. Distance and Directional Analyses of Settlement Patterns. Economic Geography 62, 167-179.
- Vernon, P., 1966. Drumlins and Pleistocene Ice Flow over the Ards Peninsula/Strangford Lough Area, County Down, Ireland. Journal of Glaciology 6, 401-409.
- Vilborg, L., 1977. The Cirque Forms of Swedish Lapland. Geografiska Annaler A59, 89-150.
- Vincent, P.J., 1987. Spatial Dispersion of Polygonal Karst Sinks. Zeitschrift für Geomorphologie 31, 65-72.
- Williams, P.W., 1971. Illustrating Morphometric Analysis of Karst with Examples from New Guinea. Zeitschrift für Geomorphologie 15, 40-61.
- Williams, P.W., 1972. The Analysis of Spatial Characteristics of Karst Terrains. In Chorley, R.J. (ed): Spatial Analysis in Geomorphology. Harper & Row, New York.
- Williams, P.W., 1972. Morphometric Analysis of Polygonal Karst in New Guinea. Geological Society of America, Bulletin 83, 761-796.